Integrated system for temperature-controlled fast protein liquid chromatography. III. Continuous downstream processing of monoclonal antibodies

Ketterer, Benedikt; Moore-Kelly, Charles; Thomas, Owen; Franzreb, Matthias

DOI:
10.1016/j.chroma.2019.460429

Document Version
Peer reviewed version

Citation for published version (Harvard):
Ketterer, B, Moore-Kelly, C, Thomas, O & Franzreb, M 2019, 'Integrated system for temperature-controlled fast protein liquid chromatography. III. Continuous downstream processing of monoclonal antibodies', *Journal of Chromatography A*, vol. 1609, 460429. https://doi.org/10.1016/j.chroma.2019.460429

Elsevier Editorial System(tm) for Journal of Chromatography A

Manuscript Draft

Manuscript Number:

Title: Integrated system for temperature-controlled fast protein liquid chromatography. III. Continuous downstream processing of monoclonal antibodies

Article Type: Full length article

Keywords: Bioseparation;
buffer exchange;
continuous chromatography;
immunoglobulins;
protein A/G affinity;
thermoresponsive ligands

Corresponding Author: Professor Matthias Franzreb, Prof. Dr.-Ing.

Corresponding Author's Institution: Karlsruhe Institut für Technologie

First Author: Benedikt Ketterer

Order of Authors: Benedikt Ketterer; Charles Moore-Kelly; Owen R. T. Thomas; Franzreb Matthias

Abstract: Three different applications, i.e. continuous concentration, quasi-continuous separation and quasi-continuous buffer exchange, of travelling heating zone reactor (THZR) chromatography for the downstream processing of monoclonal antibodies (mAbs), are described. MAb containing feedstocks were applied to a fixed bed of the commercial thermoresponsive rProtein A matrix, Byzen Pro™, contained in a bespoke stainless steel thin-walled column (held at 15°C) fitted with a travelling heating (42°C) device (a special assembly of Peltier elements and copper blocks) encircling a narrow section of the column. For the demonstration of continuous mAb concentration, uninterrupted loading of 1.0 g/L mAb in a HEPES binding buffer (20 mM HEPES, 150 mM NaCl, pH 8) was synchronized with five repeated movements of the heating zone along the column's full length at a velocity of 0.1 mm/s. Elution of bound mAbs from the column was induced solely by the travelling heating zone's action, each full movement generating a sharp concentrated elution peak accompanied by a small transient mAb concentration-dependent dip in conductivity. From the third movement of the heating zone on quasi-steady-state operation ensued; the mean eluted mAb concentration and process yields from the last three heating zone movements were respectively 4.9 ± 0.2 g/L and >93%. Quasi-continuous separation of the target mAb from the non-binding impurity (bovine serum albumin, BSA), was achieved by cyclically alternating the feeding of a two-component feedstock (1.41 g/L mAb + 1.0 g/L BSA in binding buffer) to the column, with that of the binding buffer alone (20 mM sodium phosphate, 150 mM NaCl, pH 8 binding buffer); supply of the latter was timed to coincide with movement of the heating zone. Accurate coordination of the heating zone's travel and switching from feed to buffer permitted quasi-steady-state collection, again from the third to the last THZ pass (i.e. elutions 3 - 6), of sharp peaks of mAb in high purity (98.7%) and yield (88.7%) in 4.5-fold concentrated form,

with BSA exiting the column in the flow through fractions between successive mAb elution peaks. Fully automated THZR-mediated quasi-continuous buffer exchange of 1.34 g/L mAb from a 20 mM sodium phosphate, 150 mM NaCl, pH 8 binding buffer into a new buffer of slightly lower conductivity (20 mM HEPES, 150 mM NaCl, pH 8) was performed over a 19 h period in a manner similar to that described for separation of mAb from BSA, i.e. by carefully timed switching from one feed solution to the other and back again, whilst synchronising movement of the heating zone with feeding of the exchange buffer. Quasi-steady-state operation (elutions 2 - 9) resulted in an average eluted mAb yield of 94.5% and concentration of 4.8 ± 0.1 g/L. Triggering movement of the heating zone slightly ahead of the switch from mAb feed to exchange buffer (effectively uncoupling elution from changes to mobile phase composition) permitted the positioning of mAb elution peaks in 9 mL volume segments with the lowest recorded conductivity. Measurements of buffer exchange performance conducted with two 'protein-free' systems (i.e. 1 M NaCl exchanged with water; 20 mM sodium phosphate, 150 mM NaCl, pH 8 exchanged with 20 mM HEPES, 150 mM NaCl, pH 8) demonstrated that compared to 'state-of-the-art' tangential flow filtration in diafiltration mode the THZR chromatography based approach affords a >60% saving in minimum volume of exchange buffer required to remove 99.9% of the original buffer. Combined far and near UV circular dichroism, intrinsic fluorescence and thermal melting experiments showed that, unlike conventional Protein A/G affinity chromatography, the conditions for THZR Protein A chromatography respect maintenance of a favourable structural profile for mAbs.

Suggested Reviewers: Egbert Müller
Tosoh Bioscience
egbert.mueller@tosoh.com
Egbert Müller is a proven expert for chromatography and especially for chromatographic media.

Daniel Bracewell
UCL Department of Biochemical Engineering
d.bracewell@ucl.ac.uk
Daniel Bracelwell’s research focuses on bioprocess analysis and downstream processing of biopharmaceuticals.

William Lewis
GlaxoSmithKline
william.j.lewis@gsk.com
William Lewis works in biopharmaceutical process development and intensification. In particular, he is a specialist for antibody products.

Simone Dimartino
The University of Edinburgh
Simone.Dimartino@ed.ac.uk
Simone Dimartino's expertise lies in the field of bioseparation and in particular in the design and development of novel chromatographic stationary phases.

Opposed Reviewers:

Dear Editors,

We are writing to ask you to consider our manuscript entitled '*Integrated system for temperature-controlled fast protein liquid chromatography. III. Continuous downstream processing of monoclonal antibodies'* for publication in the Journal of Chromatography A. We believe this work fits the Journal's scope perfectly, and that it will be of great interest to its readers, especially those involved in the development of new chromatographic materials, column hardware and chromatographic processes, for the recovery and purification of macromolecular target molecules.

There is strong interest in employing continuous chromatography for monoclonal antibody (mAb) capture and purification. Although impressive cost and productivity savings have been reported 'core problems' persist, namely the use of large volumes of buffer for equilibrating, washing, eluting and cleaning of columns, generating as a consequence excessive quantities of waste. Moreover, the harsh low pH elution conditions typically employed to desorb mAb from Protein A/G affinity columns can result in denaturation and aggregation. Effective solutions to these significant problems have not yet been forthcoming, but would clearly make for leaner, greener and more sustainable manufacturing of mAbs and other valuable bioproducts.

Looking to the longer term future of bioprocess-scale adsorption chromatography, we recently introduced a new scaleable continuous chromatography format 'Travelling Cooling/Heating Zone Reactor (TCZR/THZR) Chromatography' *employing a single column operated isocratically*[1,2]. In TCZR/THZR chromatography discrete 'local' changes in temperature are used to control adsorption–desorption equilibria; this is achieved through combined use of thermoresponsive chromatographic supports and a novel device (a travelling cooling or travelling heating zone reactor) that permits continuous thermally mediated desorption from the support. Our previous demonstrations of the concept have employed thermoresponsive ion exchange media and TCZR. The first study described the design/construction of the TCZR system, fabrication of thermoresponsive cation exchangers, batch-mode TCZR chromatography trials, and identified intra-particle diffusion and the ratio between the velocities of the cooling zone and mobile phase as key parameters affecting TCZR chromatography performance[1]. In the second work, we advanced TCZR chromatography further developed, illustrating the importance of short diffusion paths and sufficiently large pores for optimal TCZ elution, and demonstrating successful use of TCZR for quasi-continuous steady-state accumulation and concentration of the target binding species (lactoferrin), and its continuous separation from a non-binding protein, bovine serum albumin[2].

In this third study, using a commercially available thermoresponsive rProtein A matrix displaying reduced binding at elevated temperatures, we illustrate three different applications of continuous THZR-based chromatography for the downstream processing of mAbs, i.e. for:

---

[1] T.K.H. Müller, P. Cao, S. Ewert, J. Wohlgemuth, H. Liu, T.C. Willett, E. Theodosiou, O.R.T. Thomas, M. Franzreb, Integrated system for temperature-controlled fast protein liquid chromatography comprising improved copolymer modified beaded agarose adsorbents and a travelling cooling zone reactor arrangement, J. Chromatogr. A. 1285 (2013) 97–109. doi:10.1016/j.chroma.2013.02.025

[2] P. Cao, T.K.H. Müller, B. Ketterer, S. Ewert, E. Theodosiou, O.R.T. Thomas, M. Franzreb, Integrated system for temperature-controlled fast protein liquid chromatography. II. Optimized adsorbents and 'single column continuous operation', J. Chromatogr. A. 1403 (2015) 118–131. doi:10.1016/j.chroma.2015.05.039

(i) continuous isocratic concentration of mAbs; (ii) continuous separation and concentration of mAbs away from a non-binding impurity; and (iii) continuous buffer exchange.

We confirm that the work is new and original and that the article is not submitted or published elsewhere. We hope you will consider our manuscript worthy of publication and we look forward to the results of the review process.

Yours sincerely,

The corresponding authors (Profs Owen R.T. Thomas and Matthias Franzreb)

Highlights

- gentle mAb purification using thermoresponsive chromatography
- three applications of a novel travelling heating zone reactor (THZR)
- continuous mAb concentration (~5 fold), high yield of >93%
- quasi-continuous mAb separation from a second component with high purities (>98%)
- quasi-continuous buffer exchange, demonstrating potential exchange buffer savings

Integrated system for temperature-controlled fast protein liquid chromatography. III. Continuous downstream processing of monoclonal antibodies

Benedikt Ketterer[a], Charles Moore-Kelly[b], Owen R. T. Thomas[b,*], Matthias Franzreb[a,**]

[a]Institute for Functional Interfaces, Karlsruhe Institute of Technology, Hermann-von-Helmholtz-Platz 1, 76344 Eggenstein-Leopoldshafen, Germany

[b]School of Chemical Engineering, College of Engineering and Physical Sciences, University of Birmingham, Edgbaston, Birmingham B15 2TT, England, UK

Keywords: Bioseparation; buffer exchange; continuous chromatography; immunoglobulins, protein A/G affinity; thermoresponsive ligands

*Corresponding author. Tel.: +44 121 4145278; fax: +44 121 4145377

**Corresponding author. Tel.: +49 721 608 23595; fax: +49 721 608 23478

E-mail addresses: o.r.t.thomas@bham.ac.uk (O.R.T. Thomas); matthias.franzreb@kit.edu (M. Franzreb)

Abstract

Three different applications, i.e. continuous concentration, quasi-continuous separation and quasi-continuous buffer exchange, of travelling heating zone reactor (THZR) chromatography for the downstream processing of monoclonal antibodies (mAbs), are described. MAb containing feedstocks were applied to a fixed bed of the commercial thermoresponsive rProtein A matrix, Byzen Pro™, contained in a bespoke stainless steel thin-walled column (held at 15°C) fitted with a travelling heating (42°C) device (a special assembly of Peltier elements and copper blocks) encircling a narrow section of the column. For the demonstration of continuous mAb concentration, uninterrupted loading of 1.0 g/L mAb in a HEPES binding buffer (20 mM HEPES, 150 mM NaCl, pH 8) was synchronized with five repeated movements of the heating zone along the column's full length at a velocity of 0.1 mm/s. Elution of bound mAbs from the column was induced solely by the travelling heating zone's action, each full movement generating a sharp concentrated elution peak accompanied by a small transient mAb concentration-dependent dip in conductivity. From the third movement of the heating zone on quasi-steady-state operation ensued; the mean eluted mAb concentration and process yields from the last three heating zone movements were respectively 4.9 ± 0.2 g/L and >93%. Quasi-continuous separation of the target mAb from the non-binding impurity (bovine serum albumin, BSA), was achieved by cyclically alternating the feeding of a two-component feedstock (1.41 g/L mAb + 1.0 g/L BSA in binding buffer) to the column, with that of the binding buffer alone (20 mM sodium phosphate, 150 mM NaCl, pH 8 binding buffer); supply of the latter was timed to coincide with movement of the heating zone. Accurate coordination of the heating zone's travel and switching from feed to buffer permitted quasi-steady-state collection, again from the third to the last THZ pass (i.e. elutions 3 – 6), of sharp peaks of mAb in high purity (98.7%) and yield (88.7%) in 4.5-fold concentrated form, with BSA exiting the column in the flow through fractions between successive mAb elution peaks. Fully automated THZR-mediated quasi-continuous buffer exchange of 1.34 g/L mAb from a 20 mM sodium phosphate, 150 mM NaCl, pH 8 binding buffer into a new buffer of slightly lower conductivity (20 mM HEPES, 150 mM NaCl, pH 8) was performed over a 19 h period in a manner similar to that described for separation of mAb from BSA, i.e. by carefully timed switching from one feed solution to the other and back again, whilst synchronising movement of the heating zone with feeding of the exchange buffer. Quasi-steady-state operation (elutions 2 – 9) resulted in an average eluted mAb yield of 94.5% and concentration of 4.8 ± 0.1 g/L. Triggering movement of the heating zone slightly ahead of the switch from mAb feed to exchange buffer (effectively

uncoupling elution from changes to mobile phase composition) permitted the positioning of mAb elution peaks in 9 mL volume segments with the lowest recorded conductivity. Measurements of buffer exchange performance conducted with two 'protein-free' systems (i.e. 1 M NaCl exchanged with water; 20 mM sodium phosphate, 150 mM NaCl, pH 8 exchanged with 20 mM HEPES, 150 mM NaCl, pH 8) demonstrated that compared to 'state-of-the-art' tangential flow filtration in diafiltration mode the THZR chromatography based approach affords a >60% saving in minimum volume of exchange buffer required to remove 99.9% of the original buffer. Combined far and near UV circular dichroism, intrinsic fluorescence and thermal melting experiments showed that, unlike conventional Protein A/G affinity chromatography, the conditions for THZR Protein A chromatography respect maintenance of a favourable structural profile for mAbs.

1. Introduction

The global market for biopharmaceuticals is strong (US$230 billion in 2016) and year-on-year growth is exceedingly healthy [1-3]. Recombinant protein therapeutics account for nearly 70% of the biopharma market share [1], and within this grouping monoclonal antibody (mAb) based drugs, an intensely studied, hugely important class of biotherapeutics capable of targeting disease cells, blocking cellular signalling pathways or transporting conjugated cytotoxic agents to disease tissues [4,5], are dominant. The current global market value for mAbs in clinical use of more than US$100 billion is predicted to reach US$130-200 billion by 2022 [6]. To keep up with market demand many big biopharma companies have invested in large production plants, employing hard-piped equipment, stainless steel bioreactors and holding tanks, operating standardized platform processes. Increasingly however, the need to reduce production costs in biopharmaceutical manufacturing becomes pressing, driven by: rising markets for personalized medicines; growing adoption of single-use disposables technologies; smaller, leaner, flexible and portable production facilities on the rise; increased product titres; and knowledge that new approaches with the potential to significantly boost productivity, are emerging – principal among these being continuous processing techniques [7-9].

Several comprehensive studies, most in the context of mAb manufacture, highlight the impressive cost savings and operational advantages expected on transitioning from conventional batch processing to fully integrated continuous or hybrid batch-continuous manufacturing approaches [10-13], and recent experimental demonstrations of 'end-to-end' processes go some way to confirming expectations [8,14-16]. Continuous chromatography

systems feature at the heart of these manufacturing platforms, and employ the common approach of operating multiple smaller columns in parallel or concurrently [17-20]. Although significant cost and productivity savings have been reported, 'core problems' persist, namely the use of large volumes of buffer for equilibrating, washing, eluting and cleaning of columns, generating as a consequence excessive quantities of waste. Moreover, the harsh low pH elution conditions typically employed to desorb mAb from Protein A/G affinity columns can result in denaturation and aggregation [21,22]. Effective solutions to these significant problems have not yet been forthcoming, but would clearly make for leaner, greener and more sustainable manufacturing of mAbs and other valuable bioproducts.

The advent of chromatography matrices that permit elution of bound protein targets by means of temperature shift raises interesting prospects for the purification of mAbs and similarly heat stable proteins [23-25]. One such matrix, Byzen Pro™ is a commercial resin that employs a thermoresponsive mutant of Protein A ligand, which provides an alternative elution method; binding is conducted at low temperature (*ca.* 10°C) and near neutral pH and elution is achieved by raising the temperature to 37-40°C without altering the mobile phase composition. The thermoresponsive properties of the ligand were engineered by introducing mutations to reduce the hydrophobicity of residues buried within the core of the IgG-binding domain, resulting in a destabilised structure that exhibits a shift of folding equilibrium across a relatively narrow temperature range [23].

The temperature switching bind-elute format of thermoresponsive resins is particularly interesting as it invites new modes of chromatographic operation. We recently introduced a new scalable continuous chromatography 'Travelling Cooling/Heating Zone Reactor' (TCZR/THZR) Chromatography', which employs a single column operated isocratically [24,25]. In TCZR/THZR chromatography discrete 'local' changes in temperature are used to control 'adsorption–desorption' equilibria. This is achieved through combined use of thermoresponsive chromatographic supports packed in a thin-walled stainless-steel column and a novel device (a travelling cooling or heating zone reactor; TCZ or THZ) girdling a narrow section of the column that permits continuous thermally mediated desorption from the support. In standard batch wise operation, feedstock is applied to the column at a particular temperature (elevated for TCZR and reduced for THZR operation). Once loading is complete, the column is washed with an equilibration buffer at the same temperature, and the TCZ/THZ is simultaneously moved along the column's full length (multiple times) in the direction of the mobile phase at a velocity much lower than that of interstitial mobile phase. Each arrival of TCZ/THZ at the column exit is heralded by generation of a sharp concentrated elution

peak. In our past work [24,25] we employed TCZR chromatography with thermoresponsive cation exchange media displaying reduced target (lactoferrin) binding at low temperature. While the first study described the design/construction of the TCZR system, fabrication of thermoresponsive cation exchangers, batch-mode TCZR chromatography trials, and identified intra-particle diffusion and the ratio between the velocities of the cooling zone and mobile phase as key parameters affecting TCZR chromatography performance [24], the second pushed the advance TCZR further, by illustrating the importance of short diffusion paths and sufficiently large pores for optimal TCZ elution, and demonstrating successful use of TCZR for quasi-continuous steady-state accumulation and concentration of the target binding species (lactoferrin) and also its continuous separation from the non-binding protein, bovine serum albumin [25].

The opposite case of employing THZR chromatography with adsorbents exhibiting reduced binding at elevated temperatures, originally broached by Müller et al. [24], is described in this study. Here we illustrate three different applications of continuous THZR-based rProtein A affinity chromatography for the downstream processing of mAbs. First, for continuous isocratic concentration of mAbs. Here, the incoming feed of constant mAb titre is fractionated into sharp concentrated peaks, which can be pooled at regular intervals by means of a two-way valve. Second, for continuous separation and concentration of mAbs away from non-binding impurities. For this the incoming flow of mAb is interrupted at short intervals with a slug of a buffer of choice. The intervals are tightly synchronised with movements of the THZ so that eluted concentrated mAb is placed into a new buffer. Third, for continuous buffer exchange by alternately flipping the incoming flow back and forth between mAb feed and exchange buffer, delivering a fast and efficient process that uses far less buffer than conventional ultra-/diafiltration systems.

2. Experimental

2.1 Materials

Byzen Pro™ temperature-responsive Protein A resin used in THZR experiments and 1 mL HiTrap Protein G HP columns employed for determination of mAb purity, were purchased from Sigma Aldrich (Taufkirchen, Germany) and GE Healthcare (Uppsala, Sweden) respectively. IgG_1 mAbs were kindly provided by Novartis AG (Basel, Switzerland) and Pall Life Sciences (Portsmouth, Hants, UK). Sodium dihydrogen phosphate dihydrate, sodium chloride, urea, sodium hydroxide (1 M) and glycine were purchased from Merck KGaA

(Darmstadt, Germany). Bovine serum albumin (heat shock fraction, protease free, fatty acid free, essentially globulin free, ≥98%), HEPES and phosphate assay kit (MAK308) were purchased from Sigma Aldrich. Citric acid monohydrate, trisodium citrate dihydrate were obtained from BDH Laboratory Supplies (Poole, Dorset, UK), and hydrochloric acid (~37%), sodium dihydrogen orthophosphate dihydrate and anhydrous di-sodium hydrogen orthophosphate were supplied by Fisher Scientific UK Ltd. (Loughborough, Leics, UK). All solutions were prepared using deionized water purified using arium® pro VF (Sartorius, Göttingen, Germany) or PURELAB® Option-R Ultra (ELGA LabWater, High Wycombe, UK) water purifications systems.

2.2 Travelling heating zone reactor (THZR) chromatography

The travelling heating zone reactor (THZR) chromatograph system employed in this work is largely based on the design of the travelling cooling zone reactor (TCZR) set-up we described previously [24,25], featuring a movable cooling device surrounding a discrete zone of a bespoke fixed bed column. The main differences between the new THZR (Fig. 1) and earlier TCZR systems centre on the construction of a temperature-controlled box for cooling the separation column (Fig. 1a); and of a movable heating zone (Fig. 1b). The central part of the THZR is a bespoke thin-walled (1 mm thick) narrow-bored column (i.d. = 6 mm) fabricated out of stainless steel (to ensure good heat conductance through the walls). Two adaptors inserted into the column are used to contain fixed beds of an appropriate thermoresponsive chromatography matrix, e.g. Byzen Pro™. The column is boxed within a housing insulated with rubber mats, and the box's interior temperature is adjusted by means of a Peltier cooling/heating unit (model UEPK-A2AH-24V-215W) and Peltier temperature controller (model UETR-MOST-16A); both obtained from Uwe Electronic GmbH (Unterhaching, Germany). The heating zone assembly (Fig. 1b) comprises a central Peltier element sandwiched between two copper blocks of differing thickness, i.e. (i) an upper 3 cm thick copper block heated via the hot face of a Peltier element (Type TB-109-1,4-1,5CH, Kryotherm, St. Petersburg, Russia), the latter being connected to a Peltier controller (Model MTTC-1410, Laird Technologies, Chesterfield, MO, USA), with its thermocouple inserted into a hole within the upper copper block; and (ii) a lower 0.5 cm thick copper block. The copper blocks are fixed between two specially modified aluminium heat sinks with attached CPU coolers (LA-6-100-12, Fischer Elektronik, Lüdenscheid, Germany), and the upper copper block is thermally insulated from the ambient air and from the assembly's upper heat sink. While the upper heat sink affords cooling of a previously heated area of the column, the

lower heat sink/ cooler prevents overheating of the Peltier element. Movement of the THZ is achieved by attaching the unit to an electric slide with ball screw drive (EGSK-33-600-6P) powered by a Servo motor (EMMS-AS-40-M-TMB), controlled by dedicated Festo Configuration Tool (FCT) PC based software (Festo AG, Munich, Germany). The THZR column is connected to an Äkta Purifier 10 (GE Healthcare, Uppsala, Sweden) FPLC system.

2.3 Chromatography experiments with the THZR

2.3.1 General procedure for chromatography with the THZR

Fixed beds (V = 6.2 mL, h = 22 cm) of Byzen Pro™ matrix were used in all experiments. The temperatures of the reactor housing the column and of the THZ were set to 15 and 42°C respectively and were measured continuously throughout experiments by means of Pt 100 thermocouples linked to LabView Software (National Instruments, Austin, TX, USA). In all experiments, feeds and buffer solutions were applied at a constant flow rate of 30 mL/h (106.1 cm/h or 0.3 mm/s) to the inlet at the upper end of the column. For temperature-induced elutions, the heating zone was moved down the column slowly at a velocity of just 0.1 mm/s. The downward movement lasted 1 h, starting at the top of the adsorbent bed and ending at an 'idle position' sufficiently far distanced (14 cm) below the end of the particle bed to eliminate heat transfer to the thermoresponsive medium between successive temperature-induced elutions. Before each downward travel the heating zone was rapidly moved (40 mm/s, 9 s) up the column to its starting position. The UV absorbance of the effluent was measured online at 300 nm, and all fractions generated during experiments were retained for off-line analysis (see 2.6). Residually bound protein was desorbed by stripping with 8 M urea to ensure constant starting conditions between experiments.

2.3.2 Example 1: Continuous concentration of mAbs

Three hundred and fifty millilitres of 1.0 g/L mAb in 20 mM HEPES pH 8 buffer supplemented with 150 mM NaCl was loaded onto the Byzen Pro™ column pre-equilibrated with the same buffer. During this period, the heating zone was periodically moved down the column. Five movements were performed in all, the first was started 227 min into loading, and the rest were initiated at ~100 min intervals thereafter, i.e. at 327, 427, 528 and 628 min.

2.3.3 Example 2: Quasi-continuous separation of mAbs from a non-binding protein impurity

One hundred millilitres of a synthetic binary protein feed solution of mAb (1.41 g/L) and BSA (1.00 g/L) suspended in 20 mM sodium phosphate, 150 mM NaCl, pH 8 buffer was applied to a Byzen Pro™ column equilibrated in the same buffer. This was followed by five cycles of 25 mL fresh buffer and 35 mL of the mAb/BSA cocktail, and a sixth of 25 mL fresh buffer and just 20 mL of mAb/BSA feed. Movements of the heating zone were started after 214, 329, 454, 574, 694, 815 and 935 min.

2.3.4 Example 3: Quasi-continuous buffer exchange

In the first experiment, 100 mL of 1.34 g/L mAb suspended in 20 mM sodium phosphate, 150 mM NaCl pH 8 was loaded onto an equilibrated Byzen Pro™ column. This was followed by nine alternating cycles of 20 mM HEPES, 150 mM NaCl, pH 8 exchange buffer (20 mL) and then mAb solution (35 mL for the first 8 applications and 15 mL in the ninth). Nine THZ movements were performed starting at 214, 319, 429, 539, 650, 760, 870, 980 and 1090 min into the run.

A second buffer exchange experiment was conducted following constructive modifications to the column to minimize the dead volume in front of the bed. The column was supplied with 100 mL of 1.39 g/L mAb in the same buffer, before applying six successive cycles of the exchange buffer (25 mL) and feed (35 mL for the first five applications and 20 mL for the sixth). Six THZ movements were carried out (in this experiment from a starting position 4 cm above the top of the adsorbent bed) after 208, 328, 449, 569, 689 and 809 min.

2.4 Evaluation of process performance

Process performance was assessed by analysing the mAb concentrations of collected fractions (see 2.6). The concentration factor achieved (Eq. (1)) was calculated by dividing the average concentration of the peak (c_{peak}) by that of the incoming flow concentration (c_{inflow}).

$$f_{\mathrm{c}} = \frac{c_{\mathrm{peak}}}{c_{\mathrm{inflow}}} \quad (1)$$

The masses of mAb in fractions were determined by multiplying the mAb concentrations of fractions by their respective volumes. For the calculation of the yield per cycle ($\mathrm{Y_{cycle}}$) the inter peak flowthrough was considered as loss. $\mathrm{Y_{cycle}}$ is therefore given by

the mass of mAb in the respective peak (m_{peak}) divided by the mass of mAb in the peak plus the preceding flowthrough (m_{ft}).

$$Y_{\mathrm{cycle}} = \frac{m_{\mathrm{peak}}}{m_{\mathrm{ft}}+m_{\mathrm{peak}}} \quad (2)$$

For continuous separation of mAb from BSA the inter peak flowthrough contains both components, thus Eq. (2) cannot be applied if the protein concentrations are calculated from off-line UV measurements. In this case, for the calculation of the yield ($Y_{\mathrm{cycle,sep}}$) a mass balance of 100% is assumed, resulting in Eq. (3):

$$Y_{\mathrm{cycle,sep}} = \frac{m_{\mathrm{peak}}}{c_{\mathrm{inflow}}*\dot{V}*t} \quad (3)$$

For the mass balance of each cycle (MB) the sum of mAb in the peak and preceding flowthrough are compared with the mAb applied within the corresponding time interval (Eq. (4)).

$$\mathrm{MB}\ (\%) = \frac{m_{\mathrm{ft}}+m_{\mathrm{peak}}}{c_{\mathrm{inflow}}*\dot{V}*t} * 100 \quad (4)$$

Here $\dot{V}$ is the volumetric flow rate, and t the time interval in which mAb solution was applied. Because mass balances and yields are calculated from the mass of mAb in the flowthrough preceding each peak, it follows that these were not determined for the first peak in each experiment.

2.5 Determination of buffer exchange performance

The determination of THZR's buffer exchange performance was carried out with 'protein-free' model systems (as is standard practice) in two different ways. In both the flow rate was 30 mL/h (106 cm/h), the housing and THZ temperatures were respectively 15 and 42°C, and movement of the THZ was initiated 8 min after switching to the new exchange solvent; experiments were performed in triplicate, and all calculations were conducted using MATLAB R2017b (MathWorks, Natick, MA, USA).

In the first method, the column was first pre-equilibrated with 1 M NaCl. A 25 mL slug of deionised water was then applied, followed by 1 M NaCl to bring the bed back to its starting condition. On-line conductivity measurements performed by the FPLC system's conductivity monitor (Monitor pH/C-900, GE Healthcare, Uppsala, Sweden), were converted into NaCl concentration using the Debye-Hückel-Onsager's equation [26]. Despite the THZ's influence on local column temperature Debye-Hückel-Onsager parameters for 25 °C could be applied, because by the time exiting flow had reached the conductivity monitor its temperature was practically ambient. The mass of NaCl in the 9 mL section where the mAb

peak was determined to appear was calculated using MATLAB's trapz (trapezoidal numerical integration) function. The interval limits were varied in 1 mL steps in order to find the position of lowest NaCl concentration within the section, and the extent of NaCl removal was determined by dividing the NaCl concentration of the starting solution by that of the 9 mL section.

For the second approach, the chromatographic bed was equilibrated with 20 mM sodium phosphate, 150 mM NaCl, pH 8 buffer, loaded with 25 mL of exchange buffer (20 mM HEPES, 150 mM NaCl, pH 8), and re-equilibrated with the original buffer. One millilitre fractions were collected and assayed for phosphate content (see 2.6), and the extent of phosphate reduction in the 9 mL window into which mAb is exchanged was calculated by comparison with the starting level (20 mM phosphate) in the original buffer.

2.6 Analysis

The protein concentrations of 0.2 mL aliquots of protein solutions, appropriately diluted peak fractions, and inter-peak flow-through fractions were determined in triplicate by means of UV spectrophotometry in UV-Star UV-transparent microplates (Greiner Bio-One, Frickenhausen, Germany) at 280 nm in an Enspire Multimode plate reader (PerkinElmer, Waltham, MA, USA).

The compositions of feed solutions and peak fractions were analysed by affinity chromatography using 1 mL HiTrap Protein G HP columns and an Äkta Purifier 10 chromatography system (GE Healthcare, Uppsala, Sweden) operated at a flow rate of 60 mL/h. Samples (0.25 mL) were applied to columns pre-equilibrated with 20 mM sodium phosphate, pH 8 supplemented with 150 mM NaCl, washed with 7 CV of the same buffer, before eluting mAb with 10 CV of 100 mM glycine-HCl buffer pH 2.7. The concentrations of unbound BSA (c_{BSA}) and eluted mAb (c_{mAb}) were determined using $A^{1\%}_{280\,nm}$ values of 14.7 for mAb and 6.7 for BSA. The purity of mAb in samples was calculated as follows:

$$Purity\ (\%) = \frac{c_{\mathrm{mAb}}}{c_{\mathrm{BSA}} + c_{\mathrm{mAb}}} * 100 \qquad (5)$$

The phosphate contents of samples taken during buffer exchange experiments (see 2.5) was determined using a malachite green-based colorimetric assay kit (MAK308, Sigma-Aldrich).

Intrinsic fluorescence emission spectra were collected on 4 mg/mL mAb solutions in a 1.2 mm diameter quartz capillary flow cell [32] with an Ocean Optics HR2000+ CCD array detector and Spectra Suite™ software (Ocean Optics, Largo FL, USA). The excitation

wavelength, bandwidth and digital integration time (DIT) were 290 nm, 9 nm and 3 s respectively, and for each sample, 14 scans were accumulated before averaging.

MAb CD measurements were recorded in different elution buffers using a Jasco J-1500 CD spectrometer and Spectra Manager™ software (Jasco UK Ltd, Great Dunmow, Essex, UK). Far-UV (190 – 270 nm) measurements were made in continuous scan mode (bandwidth = 2 nm, DIT= 1 s, accumulation = 4) with 0.2 mg/mL mAb in the quartz capillary flow cell. Near-UV (230 – 330 nm) CD spectra were obtained in step scan mode (bandwidth = 2 nm, DIT = 4 s, accumulation = 4) using 0.5 mg/mL mAb in a 5 mm path length quartz cuvette. CD based thermal melts were performed with the aid of a Jasco PTC-517 Peltier thermostatted cell holder with a Jasco MCB-100 circulation bath. Melting curves were determined at 240 nm between 25 – 90ºC in thermal measurement mode (bandwidth = 2 nm, DIT = 16 s, temperature ramp rate = 5 ºC/min, temperature increment = 2 ºC) using 0.25 mg/mL mAb in rectangular quartz cells (1 cm path length). During thermal ramps, the magnetic stirrer was set to 600 rpm, the PTC-517 temperature probe was positioned in the sample, and the cuvette was sealed with a rubber cap to prevent evaporation. T_m values were obtained from the first derivative of the melting curves.

3. Results and Discussion

3.1 Example 1: Continuous concentration of mAb

The first demonstration of the THZR system for mAb downstream processing was implementation of a process for continuous concentration of the target molecule. In this process, feed solution is continuously loaded onto the column, and synchronised elution of mAb in the form of sharp concentrated peaks is achieved through repeated movements of the THZ along the full length of the column; with each travel of the device resulting in a peak. Figure 2 shows the chromatogram obtained during such a process. Each THZ movement led to a sharp elution peak (>600 mAU) with slight fronting (the result of incipient breakthrough prior to initiating THZ movement), and the UV signal of the flowthrough in between successive peaks practically returned to base line, indicating only very small losses *ergo* high process yields (Table 1).

The elution peak generated by the first THZ movement (i.e. peak 1) was much smaller than that of all subsequent passes of the THZ (peaks 2–5), and quasi-steady-state appeared to be reached with the third movement of the THZ (~1200 mAU for peaks 3–5). The practically constant conductivity profile derives from the use of a constant mobile phase composition

throughout the experiment (an elution buffer was not used). Elution was induced solely by travel of the heating zone along the column, and the observed small drops in conductivity coincided with and were related to the mAb concentrations of the eluting peaks (conductivity dropped from ~15.2 to 15.1 mS/cm for peak 1, and further to 14.9 mS/cm for peaks 3–5). Quantitative analysis (Table 1) confirms that steady-state operation is achieved with the third THZ pass (the mAb content of elution peaks 3–5 were 44.8 ± 2.2 mg *cf.* 18.5 and 39.9 mg for peaks 1 and 2 respectively). The summated mass of the steady-state peaks 3, 4 and 5 (134.3 mg) equates to >93% yield, a mass balance closure of nearly 96%, and a near five-fold concentration of mAb.

3.2 Example 2: Quasi-continuous mAb purification from a non-binding impurity

Defining appropriate operating conditions for THZR-mediated quasi-continuous chromatographic purification of a target binding protein from a non-binding protein impurity requires a sound understanding of the idea, principles and parameters involved. A schematic illustration of the concept, highlighting profiles for both the mobile phase concentrations of the binding target and non-binding species, and stationary phase target loading, is shown in Fig 3. Key assumptions are that: (i) the adsorption and desorption of target depends solely on the temperature; and (ii) the impurity does not bind to the matrix, regardless of the prevailing temperature.

An individual operating cycle in THZR chromatography comprises four sequential phases. The first two differ little from conventionally applied FPLC (tight control of the column temperature in THZR chromatography is atypical). With the THZ parked well away (14 cm) from the fixed adsorbent bed, phase 1 commences with loading of the binary component feed; the target binds and the impurity passes through the column. At this point, the stationary phase at the front of the column is loaded with target to equilibrium (indicated by the moment the front reaches column position z/z_0 ~0.5 in Fig 3, far left). The transition from phase 1 to 2 is made shortly before the mobile and stationary phase target profiles reach the column outlet (Fig. 3, left of centre). In phase 2 loading of the feed is stopped, the inflow is switched over to buffer and non-binding species are flushed out of the column. Movement of the THZ is initiated during phase 3, creating an elution peak and increasing stationary phase target loading in sections of the column being located directly downstream of the THZ (indicated by z/z_0 ~0.25; Fig. 3, right of centre) as it migrates along the column towards to the outlet. By contrast, the stationary phase target loading and mobile phase target concentrations behind the moving THZ (z/z_0 <0.2; Fig. 3, right of centre) are low (c/c_{feed} is significantly less

than 1). Clearly, temperature induced elution leads to partial recovery of the matrix's initially available capacity to bind target, so that on switching the incoming flow from buffer back to the protein feed solution (marking the transition from phase 3 to 4), a new loading front starts to form just before the elution peak exits the column (z/z_0 ~0.75; Fig. 3, far right). Phase 4 concludes shortly after the peak leaves the column, and is immediately followed by the next operation cycle, which starts with phase 1 (Fig 3, far left), i.e. reapplication of the protein feed to the adsorbent bed whilst the THZ is parked outside.

In choosing the right moment to switch the incoming flow from buffer to feed, it is important to consider that non-binding impurities travel faster through the column than the target concentration wave. The optimum time for the switch can be calculated by subtracting the mobile phase residence time from that required for the entire target peak to leave the column, which in good approximation coincides with the THZ reaching the column outlet (z/z_0 =1).

The feasibility of quasi-continuous THZR chromatography was tested for the separation of mAb (target) from BSA (non-binding impurity) using a fixed bed of Byzen Pro™ matrix and the results are presented in Fig. 4 and Table 2. In common with the continuous concentration experiment discussed earlier (see 3.1 and Fig. 2), precisely controlled timing and movement of the THZ induces sharp evenly separated near-symmetrical peaks (Fig. 4a). Immediate protein breakthrough is observed at the beginning of the process, with the UV signal hitting a plateau value consistent with the concentration of the non-binding component, BSA, in the feed (1.0 g/L) after ~2 CVs. At the end of the first loading phase, on approaching the column's maximum loading capacity for mAb, the UV absorbance starts to rise as small amounts of mAb join BSA in the exiting mobile phase. Shortly after switching the incoming flow from feed to pure buffer, the absorbance decreases as BSA entrained in the column is flushed out. As the present example shows, with the correct timing of THZ movement and switching from feed to buffer, it is possible to collect mAb eluting as sharp peaks in a highly concentrated form (Table 2) essentially free of BSA (Fig. 4b). Here, six movements of the THZ were applied, with each resulting in tall (≥1200 mAU) symmetrical elution peaks that crashed to the baseline. The UV signal of the flow through between the eluate peaks quickly returned to a roughly constant threshold of 40-45 mAU as the THZ passed the column exit and the switch back to the feed solution was made. Quasi-steady-state was reached in the third pass of the THZ (Fig. 4a, Table 2).

Figure 4b compares Protein G analyses of the binary feed solution (c_{mAb} = 1.41 g/L and c_{BSA} = 1.0 g/L) with peak number 6 from the THZR fractionation experiment (Fig. 4a).

Visual inspection of the chromatograms reveals almost complete disappearance of the flowthrough BSA peak from the THZR peak 6 sample combined with substantial growth of the eluted mAb peak. Quantitative analysis (Table 2) confirmed peak 6 mAb had been recovered in high yield (87%) and in a substantially purified (99% pure) and 4.4-fold concentrated form. Protein G chromatographic analysis of THZR peaks 3, 4 and 5 gave very similar numbers (Table 2).

3.3 Example 3: Quasi-continuous buffer exchange

The notion of performing continuous THZR chromatography whilst alternating the supply of protein feed and buffer being fed to column affords an interesting application in downstream processing, namely the potential to carry out fast and efficient buffer exchange. To demonstrate this concept a series of THZR chromatography experiments were performed with a view to transferring mAb from one buffer (e.g. 20 mM sodium phosphate, 150 mM NaCl, pH 8) into a new one of lower conductivity (e.g. 20 mM HEPES, 150 mM NaCl, pH 8) in high yield using minimal amounts of exchange buffer (Fig. 5). The buffer exchange process was followed by monitoring the conductivity of the flow exiting the column. Careful synchronisation of the timings for inflow switching and THZ movement permitted accurate placement of the eluting mAb in the exchange buffer. It should be stressed that the 20 mM HEPES, 150 mM NaCl, pH 8 buffer used for exchange does not elute bound mAb (see 3.1); elution only occurs under the THZ's influence.

In the first experiment (Fig. 5a) the elution peak retention time was adjusted following the first THZ-mediated elution (peak 1), in order to achieve a higher degree of buffer exchange in all subsequent elutions (peaks 2–9). For this, the THZ was moved 5 min earlier (relative to the buffer switch) in order to shift the position of the mAb peak into a volume segment with reduced conductivity. This highlights an attractive attribute of THZR chromatography, namely the ability to uncouple elution from events that change the mobile phase composition. The UV and conductivity traces in Fig. 5a show that quasi-steady-state is attained from peak 2 onwards; quantitative analysis of the mAb contents of the peaks and mass balancing confirms this; (Table 3).

Figure 5b shows that immediately prior to the evolution of an elution peak the conductivity falls from 16.4 to 15.4 mS/cm, and then continues to drop during THZ mediated elution, albeit less steeply, reaching a minimum value of 15.0 mS/cm precisely synchronised (volume-wise) with the elution peak's maximum, before gradually increasing back to 16.4 mS/cm on completion of the elution cycle and switching back to the mAb feed solution. The

experiment was terminated after 19.2 h, though conceivably it could have continued indefinitely. The process was fully automated (no manual adjustments were made), and mAb breakthrough in the flow though between peaks was negligible; thus mAb yield during steady-state operation (peaks 2–9) approached 95% (Table 3).

Buffer exchange performance was evaluated in greater detail (see 2.3.4), the objective being to determine the efficiency of buffer exchange achievable when 25 mL slugs of exchange buffer are used for each mAb elution peak of 9 mL volume (calculated from Fig. 5). Two different tests with protein-free model systems were conducted. In the first of these 1 M NaCl was used as the feed solution (instead of mAb in 20 mM sodium phosphate, 150 mM NaCl, pH 8) and deionised water was employed in place of the exchange buffer (20 mM HEPES, 150 mM NaCl, pH 8). On-line conductivity measurements of the exiting flow were converted into NaCl concentration, which permitted calculation of the degree of buffer exchange that had been achieved (see 2.5). Figure 6a shows that the conductivity crashes steeply reaching its lowest values (0.25 - 0.06 mS/cm) over the 9 mL section corresponding to where the mAb elution peak should occur, equating to the removal of 99.94% of the initial feed solution (1 M NaCl).

In the second test, 20 mM sodium phosphate, 150 mM NaCl, pH 8 buffer was exchanged against 20 mM HEPES, 150 mM NaCl, pH 8. On-line monitoring of conductivity during the exchange process (Fig. 6b) showed a fall from 17.2 mS/cm before exchange, to a stable 15.7 mS/cm across the 9 mL section of exchange buffer into which mAb is eluted by the THZ, and off-line determination of the phosphate concentration (see 2.5 and 2.6) confirmed 99.93% removal of the original buffer (14.1 μM equating to 1,377 fold dilution of the feed). With ‘state-of-the-art’ tangential flow filtration (TFF) operated in diafiltration mode the theoretical minimum volume of exchange buffer required to deliver 99.9% removal of the original buffer of 6.9 times that of the product [27] is much higher than the 2.8 times practically observed for the quasi-continuous THZR system demonstrated herein, representing an exchange buffer volume saving of at least 60%.

Having established that a 25 mL volume of exchange buffer is sufficient to ensure >99.9% removal of the original buffer in the 9 mL putative product volume, a quasi-continuous THZR buffer exchange experiment was conducted using mAb suspended in 20 mM phosphate, 0.15 M NaCl, pH 8 and the same volume of a 20 mM HEPES, 0.15 M NaCl, pH 8 exchange buffer (Fig. 6c). Comparison of the conductivity traces in Figs 6b and 6c highlights the extra contribution of eluting mAb, i.e. a distinctive protein concentration dependent decrease in conductivity (see earlier discussion of Fig. 2) from the plateau

minimum (~15.5 mS/cm) due to the exchange buffer to new minima of ~15.1 mS/cm precisely coincident with the peak maxima, before briefly returning to the conductivity of the exchange buffer (~15.5 mS/cm). In aqueous electrolytic solutions the contribution of an ionic species to the conductivity is directly proportional to its mobility, the magnitude of which depends the size of solute ions and viscosity of the solvent [28,29], the lower the viscosity, the faster charged ions move through the medium, and vice versa. Electrical conductivity and viscosity are thus inversely correlated with one another. Hence, the observed changes in conductivity across thermally eluted mAb elution peaks (in Figs 2, 5 and 6c) likely arise from protein concentration dependent variations in the viscosity of the mobile phase.

3.4. Impact of elution buffer on mAb folding state and thermal stability

An especially attractive feature of continuous THZR mediated thermoresponsive Protein A affinity chromatography over continuous chromatographic methods employing conventional Protein A media, is that loading, washing and elution operations can all be performed with a single near neutral pH buffer. Figure 7 highlights why this is particularly advantageous. At pH 8, corresponding to 'Byzen Pro' condition, the far-UV CD profile (Fig. 7a) of mAb is that of the natively folded state, i.e. characteristic of a protein with a predominantly antiparallel ß-sheet secondary structure presenting a maximum at 203 nm and minimum at 217 nm [30], and the near-UV CD spectrum (Fig. 7b) is characterised by a peak at ≈290 nm (attributed to tryptophan), several minima between 260 – 290 nm (arising from tyrosine and phenylalanine residues), and a minimum at ~240 nm shouldering the peptide absorbing region [30,32]. In sodium citrate buffer pH 3.3 partial unfolding of mAb structure is inferred from small changes in the near-UV region below 250 nm (Fig. 7b), and far-UV CD at wavelengths below 220 nm (Fig. 7a). More severe unfolding of the peptide backbone is observed in the lower pH glycine-HCl buffers, indicated by: (i) progressive reductions in the far-UV ellipticity at 203 nm (Fig. 7a); (ii) rearrangement of aromatic residues giving a broad shift in the near-UV spectra at pH 2.7; and (iii) at pH 2.1, to changes across the entire near-UV region consistent with severe denaturation (Fig. 7b). Acid-induced unfolding of mAb was also confirmed by strong pH-dependent red-shifting of the maximum intrinsic fluorescence wavelength, from 336 nm in its native state to 342 nm at pH 2.1, as buried tryptophan residues become increasingly solvent exposed (Fig. 7c).

Figure 7d shows melting curves measured at 240 nm, a wavelength strongly indicative of important changes to mAb structural integrity [32]. The onset of melting of antibody structure is characterised by a decrease in measured ellipticity, as the random coil content

rises. At neutral pH IgGs are relatively thermostable proteins [33], exemplified here by a melting temperature (T_m) for the IgG_1 mAb of 78ºC. In stark contrast, thermal stability is seriously compromised in buffers used for elution of mAb from conventional Protein A and G columns; T_m falls to 56ºC in sodium citrate pH 3.3, 48ºC in glycine-HCl pH 2.7 and just 26ºC glycine-HCl pH 2.7 (Fig 7d).

In conclusion, the data here (Fig. 7a-d) underscore a salient advantage of continuous THZR mediated Protein A affinity chromatography over current Protein A/G affinity based approaches, namely the complete avoidance of harsh elution conditions that: (i) cause partial unfolding (perturbed ß-sheet structure, rearranged aromatic residues); (ii) reduced thermal stability; (iii) impair safety and efficacy by increasing aggregation rates post-purification [34,35]; and (iv) induce binding polyreactivity to foreign antigens [36].

4. Conclusion

A THZR chromatography system has been constructed and three applications of its use have been demonstrated in the context of quasi-continuous mAb downstream processing, i.e. concentration, purification and buffer exchange. Several unique features are identified that set THZR chromatography apart from other continuous chromatographic formats for mAbs [15,17-20], namely the abilities to:

(i) uncouple elution from events that change the mobile phase composition;

(ii) synchronise loading, buffer exchange and thermal elution in such a way that eluted mAb is placed/formulated into a buffer of choice;

(iii) outperform TFF/UF for buffer exchange [27]; and

(iv) avoid exposure of thermally tolerant but acid-labile mAbs to harsh elution conditions detrimental to maintenance of its native structure.

From an industrial perspective, however, the benefits of eluting with a favourable structural profile are likely overshadowed, at present, by a number of drawbacks related to the Byzen Pro™ matrix. These include: low mAb dynamic binding capacity (<20 mg/mL determined in this study, in good accord with refs [23] and [37]) *cf.* industry standard and 'state-of-the-art' matrices (>60 mg/mL for MabSelect SuRe™ LX and ~80 mg/mL for Praesto® Jetted A50); high salt sensitivity of the current first generation themoresponsive rProtein A ligand, which prohibits use of conventional wash steps for HCP removal [37,38]; limited flow rate range, large particle size, and poor pore diffusion [23,37] and question marks concerning extent of ligand leakage and robustness to CIP. Moreover, current platform

processes for therapeutic mAbs are locked into the use of low pH holding step for virus removal [21,39,40] despite the damage this can / is known to inflict on product antibodies [34-36]. Rather than dismiss thermally-mediated elution out of hand, a wiser proposition for the future might be to develop alternative mAb manufacturing platforms allying new 'gentle on product' replacements for the viral pH hold step [41,42] with continuous THZR chromatography employing improved thermoresponsive media.

Acknowledgements

This work was supported by the European Framework 7 large scale integrating collaborative project 'Advanced Magnetic nano-particles deliver smart Processes and Products for Life' (MagPro^{2}Life, CP-IP 229335-2) and the EPSRC Centre for Doctoral Training in Formulation Engineering (Grant number EP/L015153/1). We also thank Jonas Wohlgemuth for technical assistance with assembly of the THZR system.

References

[1] 12th Annual Report and Survey of Biopharmaceutical Manufacturing Capacity and Production, April 2015, BioPlan Associates Inc.

[2] E. Moorkens, N. Meuwissen, I. Huys, P. Declerck, A.G. Vulto, S. Simoens, The Market of Biopharmaceutical Medicines: A Snapshot of a Diverse Industrial Landscape, Front. Pharmacol. 8 (2017) 314. doi:10.3389/fphar.2017.00314

[3] H. Kaplon, J.M. Reichert, Antibodies to watch in 2019, mAbs 11(2) (2019) 219–238. doi:10.1080/19420862.2018.1556465

[4] M. Suzuki, C. Kato, A. Kato, Therapeutic antibodies: their mechanisms of action and the pathological findings they induce in toxicity studies, J. Toxicol. Pathol. 28(3) (2015) 133139. doi:10.1293/tox.2015-0031

[5] M.L. Chiu, G.L. Guilland, Engineering antibody therapeutics, Curr. Opin. Struct. Biol. 38 (2016) 163–173. doi:10.1016/j.sbi.2016.07.012

[6] A.L. Grilo, A. Mantalaris, The Increasingly Human and Profitable Antibody Market,

Trends Biotechnol. 37(1) (2019) 9–16. doi:10.1016/j.tibtech.2018.05.014

[7] A.A Shukla, U. Gottschalk, Single-use disposable technologies for biopharmaceutical manufacturing, Trends Biotechnol. 31(3) (2013) 147–154. doi:10.1016/j.tibtech.2012.10.004

[8] R. Godawat, K. Konstantinov, M. Rohani, V. Warikoo, End-to-end integrated fully continuous production of recombinant monoclonal antibodies, J. Biotechnol. 213 (2015) 13–19. doi:10.1016/j.jbiotec.2015.06.393

[9] A.A. Shukla, L.S. Wolfe, S.S. Mostafa, C. Norman, Evolving trends on mAb production processes, Bioeng. Transl. Med. 2(1) (2017) 58–69. doi:10.1002/btm2.10061

[10] A. Xenopoulos, A new, integrated, continuous purification process template for monoclonal antibodies: Process modeling and cost of goods studies, J. Biotechnol. 213 (2015) 42–53. doi:10.1016/j.jbiotec.2015.04.020

[11] J. Walther, R. Godawat, C. Hwang, Y. Abe, A. Sinclair, K. Konstantinov, The business impact of an integrated continuous biomanufacturing platform for recombinant protein production, J. Biotechnol. 213 (2015) 3–12. doi:10.1016/j.jbiotec.2015.05.010

[12] J. Pollock, J. Coffman, S. V. Ho, S.S. Farid, Integrated continuous bioprocessing: Economic, operational, and environmental feasibility for clinical and commercial antibody manufacture, Biotechnol. Prog. 33 (2017) 854–866. doi:10.1002/btpr.2492

[13] J. Hummel, M. Pagkaliwangan, X. Gjoka, T. Davidovits, R. Stock, T. Ransohoff, R. Gantier, M. Schofield, Modeling the Downstream Processing of Monoclonal Antibodies Reveals Cost Advantages for Continuous Methods for a Broad Range of Manufacturing Scales, Biotechnol. J. 1700665 (2018) 1–9. doi:10.1002/biot.201700665

[14] S. Klutz, J. Magnus, M. Lobedann, P. Schwan, B. Maiser, J. Niklas, M. Temming, G. Schembecker, Developing the biofacility of the future based on continuous processing

and single-use technology, J. Biotechnol. 213 (2015) 120–130. doi:10.1016/j.jbiotec.2015.06.388

[15] F. Steinebach, N. Ulmer, M. Wolf, L. Decker, V. Schneider, R. Wälchli, D. Karst, J. Souquet, M. Morbidelli, Design and Operation of a Continuous Integrated Monoclonal Antibody Production Process, Biotechnol. Progr. 33(5) (2017) 1303–1313. doi:10.1002/btpr.2522

[16] L. Arnold, K. Lee, J. Rucker-Pezzini, J.H. Lee, Implementation of Fully Integrated Continuous Antibody Processing: Effects on Productivity and COGm, Biotechnol. J. (2018) 1800061. doi:10.1002/biot.201800061

[17] T. Müller-Späth, G. Ströhlein, L. Aumann, H. Kornmann, P. Valax, I. Delegrange, E. Charbaut, G. Baer, A. Lamproye, M. Jöhnck, M. Schulte, M. Morbidelli, Model simulation and experimental verification of a cation-exchange IgG capture step in batch and continuous chromatography, J. Chromatogr. A 1218(31) (2011) 5195–5204. doi:10.1016/j.chroma.2011.05.103

[18] M. Bisschops, M. Brower, The impact of continuous multicolumn chromatography on biomanufacturing efficiency, Pharm. Bioprocess. 1(4) (2013) 361–372.

[19] A. Jungbauer, Continuous downstream processing of biopharmaceuticals, Trends Biotechnol. 31 (2013) 479–492. doi:10.1016/j.tibtech.2013.05.011.

[20] A.L. Zydney, Continuous downstream processing for high value biological products: A Review, Biotechnol. Bioeng. 113 (2016) 465–475. doi:10.1002/bit.25695

[21] D. Ejima, K.Tsumoto, H. Fukada, R. Yumioka, K. Nagase, T. Arakawa, J.S. Philo, Effects of acid exposure on the conformation, stability, and aggregation of monoclonal antibodies, Proteins 66(4) (2007) 954–962. doi:10.1002/prot.21243

[22] R.F. Latypov, S. Hogan, H. Lau, H. Gadgil, D. Liu, Elucidation of acid-induced unfolding and aggregation of human immunoglobulin IgG1 and IgG2 Fc, J. Biol. Chem. 287(2) (2011) 1381–1396. doi:10.1074/jbc.M111.297697

[23] I. Koguma, S. Yamashita, S. Sato, K. Okuyama, Y. Katakura, Novel purification method of human immunoglobulin by using a thermo-responsive protein A. J. Chromatogr. A. 1305 (2013) 149–53. doi:10.1016/j.chroma.2013.07.015

[24] T.K.H. Müller, P. Cao, S. Ewert, J. Wohlgemuth, H. Liu, T.C. Willett, E. Theodosiou, O.R.T. Thomas, M. Franzreb, Integrated system for temperature-controlled fast protein liquid chromatography comprising improved copolymer modified beaded agarose adsorbents and a travelling cooling zone reactor arrangement, J. Chromatogr. A. 1285 (2013) 97–109. doi:10.1016/j.chroma.2013.02.025

[25] P. Cao, T.K.H. Müller, B. Ketterer, S. Ewert, E. Theodosiou, O.R.T. Thomas, M. Franzreb, Integrated system for temperature-controlled fast protein liquid chromatography. II. Optimized adsorbents and 'single column continuous operation', J. Chromatogr. A. 1403 (2015) 118–131. doi:10.1016/j.chroma.2015.05.039

[26] P. Vanýsek, Equivalent Conductivity of Electrolytes in Aqueous Solution, in: W.M. Haynes (Ed.), Handb. Chem. Phys., 97th ed., CRC Press, Boca Raton, Florida, 2016.

[27] R.T. Kurnik, A.W. Yu, G.S. Blank, A.R. Burton, D. Smith, A.M. Athalye, R. van Reis, Buffer exchange using size exclusion chromatography, countercurrent dialysis, and tangential flow filtration: Models, development, and industrial application, Biotechnol. Bioeng. 45 (1995) 149–157. doi:10.1002/bit.260450209

[28] R.A. Horne, R.A. Courant, Application of Walden's rule to the Electrical Conduction of Sea Water, J. Geophys. Res. 69(10) (1964) 1971–1977. doi:10.1029/J2069i010p01971

[29] R.A. Horne, The Physical Chemistry and Structure of Sea Water, Water Resour. Res. 1(2) (1965) 263–276. doi:10.1029/WR001i002p00263

[30] N.J. Greenfield, Using circular dichroism spectra to estimate protein secondary structure, Nat. Protoc. 1(6) (2006) 2876–2890. doi:10.1038/nprot.2006.202

[31] A. Hawe, J. C. Kasper, W. Fries, W. Jiskoot, Structural properties of monoclonal antibody aggregates induced by freeze-thawing and thermal stress, Eur. J. Pharm. Sci. 38 (2009) 79–87. doi:10.1016/j.ejps.2009.06.001

[32] C. Moore-Kelly, Process Analytical Technology for the Manufacture of Biotherapeutic Protein Products, PhD thesis, University of Birmingham, UK, 2019.

[33] V. Irani, A.J. Guy, D. Andrew, J.G. Beeson, P.A. Ramsland, J.S. Richards, Molecular properties of human IgG subclasses and their implications for designing therapeutic monoclonal antibodies against infectious diseases, Molec. Immunol. 67(2 PtA) (2015) 171–182. doi:10.1016/j.molimm.2015.03.255.

[34] A.A. Shukla, P. Gupta, X. Han, Protein aggregation kinetics during Protein A chromatography. Case study for an Fc fusion protein, J. Chromatogr. A 1171(1-2) (2007) 22–28. doi:10.1016/j.chroma.2007.09.040

[35] A.R. Mazzer, X. Perraud, J. Halley, J. O'Hara, D.G. Bracewell, Protein A chromatography increases antibody aggregation rate during subsequent low pH virus inactivation hold, J. Chromatogr. A 1415 (2015) 83–90. doi:10.1016/*j*.chroma.2015.08.068

[36] I.K. Djoumerska-Alexieva, J.D. Dimitrov, E.N. Voynova, S. Lacroix-Desmazes, S.V. Kaveri, T.L. Vassilev, Exposure of IgG to an acidic environment results in molecular modifications and in enhanced protective activity in sepsis, FEBS J. 277(14) (2010) 3039–3050. doi:10.1111/j.1742-4658.2010.07714.x

[37] W. Krepper, P. Satzer, B.M. Beyer, A. Jungbauer, Temperature dependence of antibody adsorption in protein A affinity chromatography, J. Chromatogr. A. 1551 (2018) 59–68. doi:10.1016/j.chroma.2018.03.059

[38] S. Chollangi, R. Parker, N. Singh, Y. Li, M. Borys, Z. Li, Development of Robust Antibody Purification by Optimizing Protein-A Chromatography in Combination With Precipitation Methodologies, Biotechnol. Bioeng. 112 (2015) 2292–2304. doi:10.1002/bit.25639

[39] J.X. Zhou, in: U. Gottschalk (Ed.), Process Scale Purification of Antibodies, John Wiley and Sons, Inc., New York, 2009.

[40] Y. Li, D.W Kahn, O. Galperina, E. Blatter, R. Luo, Y. Wu, G. Zhang, in: U. Gottschalk (Ed.), Process Scale Purification of Antibodies, John Wiley and Sons, Inc., New York, 2009.

[41] H.F. Liu, J. Ma, C. Winter, R. Bayer. Recovery and purification process development for monoclonal antibody production, MAbs 2(5) (2010) 480–499. doi:10.4161/*mabs*.2.5.12645

[42] J.T. McCue, K. Selvitelli, D. Cecchini, R. Brown, Enveloped Virus Inactivation Using Neutral Arginine Solutions and Applications in Therapeutic Protein Purification Processes, Biotechnol. Prog. 30(1) (2014) 108–112. doi:10.1002/btpr.1816

Figure legends

Fig. 1. Schematic illustrations of the (a) THZR set-up and (b) its heating zone arrangement. Reactor interior temperature ~15 ºC; travelling heating zone (THZ) temperature ~42 ºC; column o.d. = 8 mm; column i.d. = 6 mm; fixed bed volume = 6.2 mL; fixed bed height ~22 cm; flow rate = 30 mL/h (106.1 cm/h); THZ velocity = 0.1 mm/s. See 2.2 and 2.3.1 for details.

Fig. 2. UV absorbance (blue) and conductivity (black) traces during THZR mediated continuous concentration of mAb from a thermoresponsive Byzen Pro™ Protein A column. MAb feed (1.0 g/L in 20 mM HEPES, 150 mM NaCl, pH 8 buffer) was continuously applied to the column (14.8 ± 0.7 ºC) during which the THZ (41.4 ± 0.06 ºC) was moved five times. The dynamic binding capacity at 0.05 g/L mAb breakthrough was 18.4 mg/mL. See 2.3.1 and 2.3.2 for experimental details.

Fig. 3. Process scheme for continuous separation of target protein from a non-binding protein impurity. The upper and lower rows respectively illustrate the mobile phase concentrations of target and impurity, and the stationary phase target loading. Each operating cycle comprises four sequential process phases as follows: initial loading of the column with feed solution (phase 1); switching the feed to pure buffer before the concentration profile reaches the outlet (phase 2); initiating THZ movement, resulting in the formation of an elution peak (phase 3); and the elution peak reaching the outlet (phase 4).

Fig. 4. Quasi-continuous THZR protein A affinity chromatography for the separation of mAb from BSA (a). MAb/BSA feed (c_{mAb} = 1.41 g/L and c_{BSA} = 1.0 g/L) was loaded onto the pre-equilibrated Byzen Pro™ column (15.2 ± 0.9 ºC), immediately followed by buffer, and then five consecutive alternating cycles of feed and buffer. Six movements of the THZ (41.4 ± 0.04 ºC) were conducted in the experiment (for details see 2.3.1 and 2.3.3). The dynamic binding capacity at 0.05 g/L mAb breakthrough was 20.0 mg/mL. (b) Protein G chromatographic analyses (see 2.6) of the mAb/BSA feed (green trace) and THZR elution peak 6 (blue trace) presented in Fig. 4a.

Fig. 5. Demonstration of THZR chromatography mediated buffer exchange experiment 1 (a) and detailed view of elution peak number 2 (b) highlighting the changes in conductivity

preceding, during and post generation elution. UV absorbance and conductivity profiles are respectively indicated by the blue and black traces in (a) and (b). MAb (1.34 g/L in 20 mM sodium phosphate, 150 mM NaCl, pH 8) was loaded onto a pre-equilbrated bed of Byzen Pro™ matrix (15.0 ± 0.9 ºC) followed by nine alternating cycles of exchange buffer (20 mM HEPES, 150 mM NaCl, pH 8) and of mAb feed. Nine movements of THZ (41.4 ± 0.04 ºC) were conducted in the experiment (for details see 2.3.1 and 2.3.4). The dynamic binding capacity at 0.05 g/L mAb breakthrough was 19.1 mg/mL.

Fig. 6. Conductivity (black traces) and UV (blue traces) during THZR mediated buffer exchange with three different systems. The temperatures of the THZ and column environment were 41.4 ± 0.05 ºC and 14.9 ± 0.8 ºC respectively. Single movements of the THZ were employed to exchange (a) 1 M NaCl with deionised water, and (b) 20 mM sodium phosphate, 150 mM NaCl, pH 8 with 20 mM HEPES, 150 mM, pH 8 buffer). Vertical grey lines in b show the individual fractions analysed for phosphate content. Dashed green lines in a and b delimit the 9 mL sections corresponding to the expected position of the mAb peak and lowest NaCl and phosphate concentrations used to calculate buffer exchange efficiencies. (c) Six THZ movements were used elute and simultaneously exchange mAb from 20 mM sodium phosphate, 150 mM NaCl, pH 8 buffer into 20 mM HEPES, 150 mM, pH 8. The dynamic binding capacity at 0.05 g/L mAb breakthrough was 13.7 mg/mL. For experimental details, see 2.3.1, 2.3.4 and 2.5.

Fig 7. (a) Far-UV CD of mAb in: 20 mM sodium phosphate, pH 8 (black); 20 mM sodium citrate, pH 3.3 (green); 20 mM glycine-HCl, pH 2.7 (blue); and 20 mM glycine-HCl, pH 2.1 (red). (b) Near-UV CD, (c) normalised fluorescence and (d) $CD_{240\ nm}$ melting curves of mAb in: 20 mM sodium phosphate, pH 8, 0.15 M NaCl (black); 100 mM sodium citrate, pH 3.3 (green); 100 mM glycine-HCl, pH 2.7 (blue); and 100 mM glycine-HCl, pH 2.1 (red).

Table 1. Evaluation of process performance during continuous concentration of mAb corresponding to Fig. 2 (see 2.3.2 and 3.1 details).

Parameter	Peak number(s)					
	1	2	3	4	5	mean 3–5 [a]
Concentration (g/L)	2.3	4.4	5.0	4.7	5.1	4.9
Concentration factor	2.3	4.4	5.0	4.7	5.1	4.9
Volume (mL)	7.9	9.0	8.9	9.1	9.1	9.1
mAb content (mg)	18.5	39.9	45.0	42.5	46.8	44.8
Yield (%)		93.2	93.4	92.7	93.3	93.1
Mass balance (%)		85.2	95.9	91.3	99.9	95.7

[a] Steady-state assumed for peaks 3 to 5.

Table 2. Evaluation of the process performance for the quasi-continuous separation shown in Fig. 4 (see 2.3.3 and 3.2 for details).

Parameter	Peak number(s)						
	1	2	3	4	5	6	mean 3–6 [a]
Concentration (g/L)	5.5	6.1	6.4	6.2	6.4	6.2	6.3
Concentration factor	3.9	4.4	4.5	4.4	4.5	4.4	4.5
Volume (mL)	7.8	6.8	7.0	6.9	6.9	6.9	6.9
mAb content (mg)	43.1	41.9	44.7	43.0	44.3	43.0	43.8
Yield (%) [b]		85.0	90.6	87.1	89.9	87.0	88.7
Purity (%)	95.6	97.1	98.1	98.5	99.0	99.0	98.7

[a] Steady-state assumed for peaks 3 to 6.
[b] Mass balance of 100% assumed.

Table 3. Evaluation of the process performance for quasi-continuous buffer exchange (experiment 1) shown in Fig. 5 (see 2.3.4 and 3.3 for details).

Parameter	Peak number(s)									
	1	2	3	4	5	6	7	8	9	mean 2-9[a]
Concentration (g/L)	3.6	4.9	4.9	4.9	4.9	4.7	4.7	4.8	4.6	4.8
Concentration factor	2.7	3.7	3.7	3.7	3.6	3.5	3.5	3.6	3.4	3.6
Volume (mL)	10.8	8.9	8.9	9.1	9.2	9.2	9.0	9.1	9.1	9.1
mAb content (mg)	39.2	43.5	44.0	44.8	44.8	43.4	42.5	43.9	41.8	43.6
Yield (%)		95.4	95.1	94.8	94.6	94.4	94.2	93.9	93.3	94.5
Mass balance (%)		97.3	98.8	100.8	101.1	98.1	96.2	99.7	95.5	98.4

[a] Steady-state assumed for peaks 2 to 9.

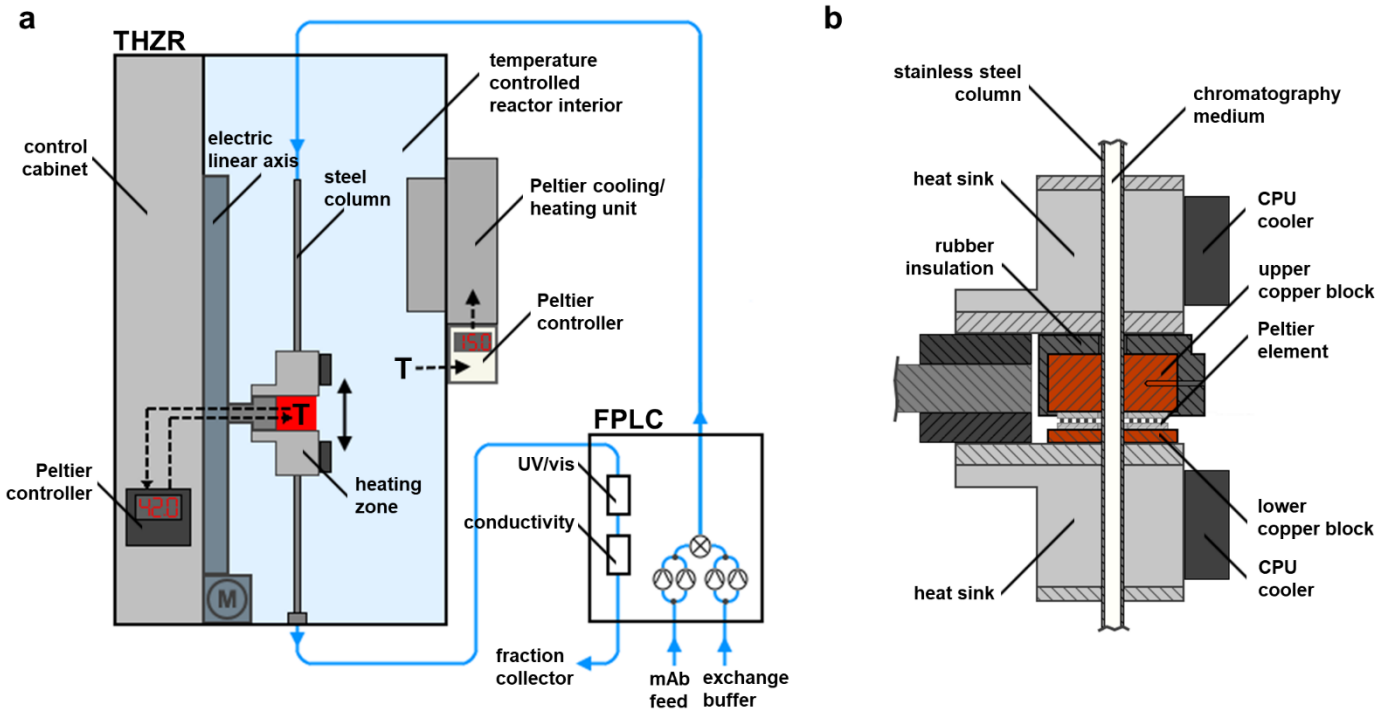

814

815 **Fig. 1.**

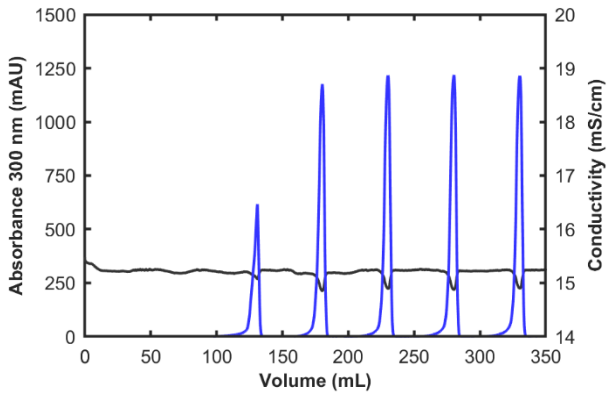

816

817 **Fig. 2.**

818

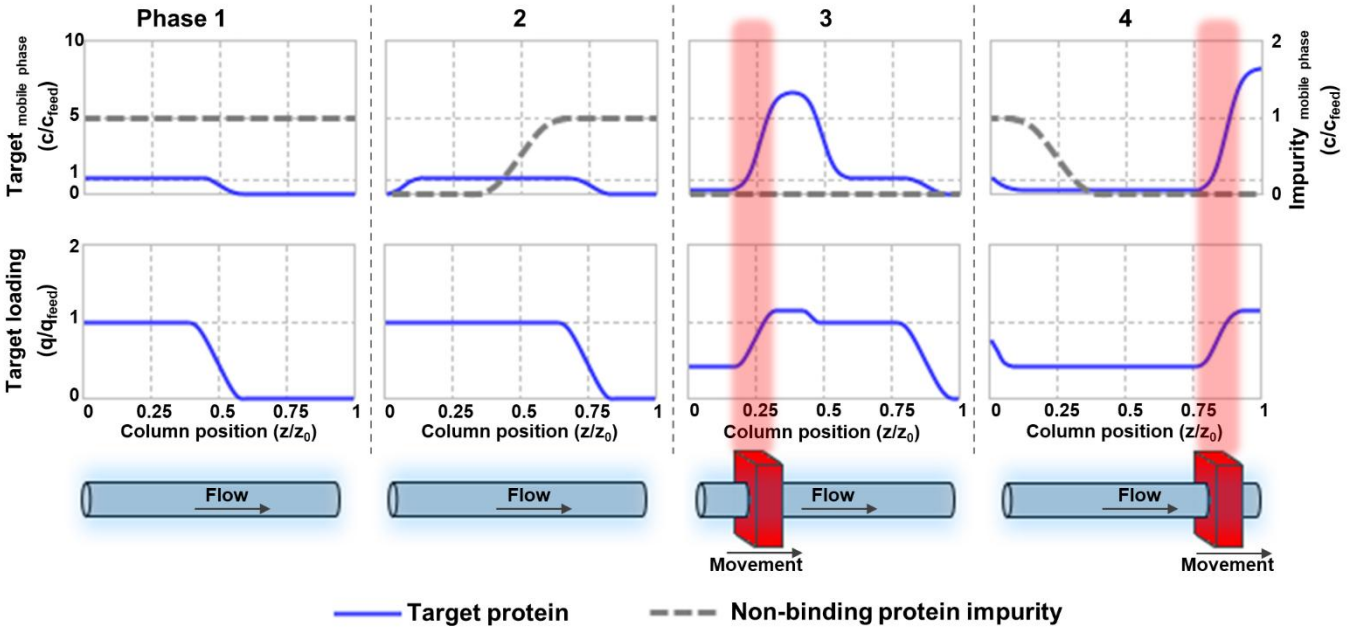

Fig. 3.

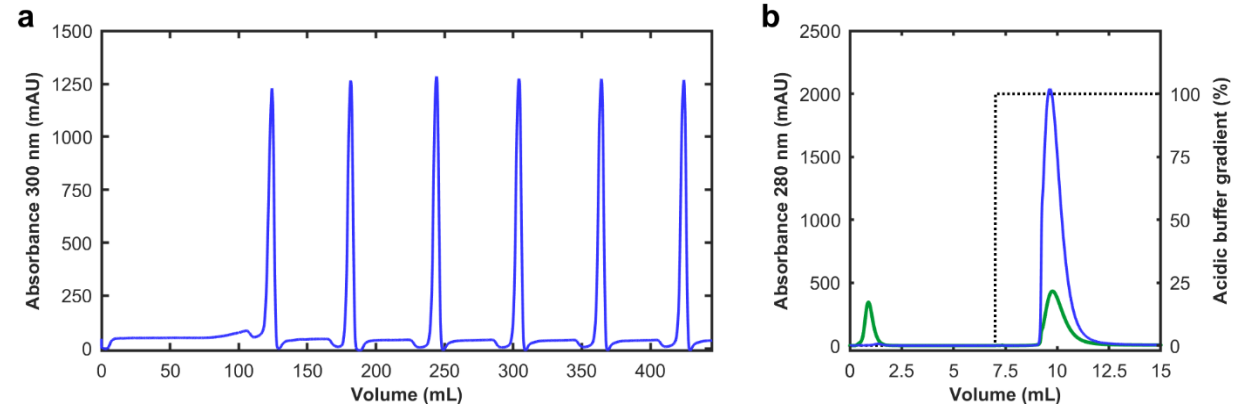

Fig. 4.

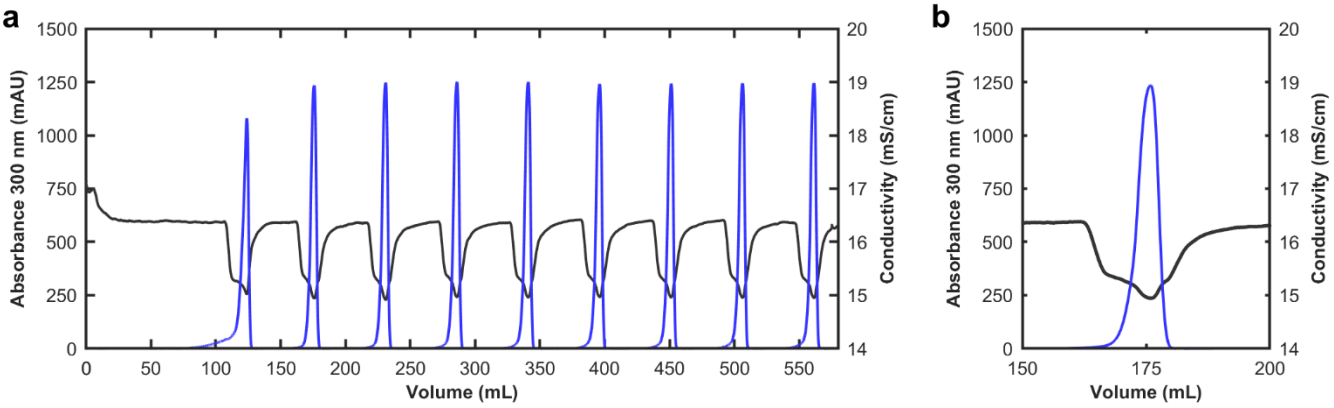

Fig. 5.

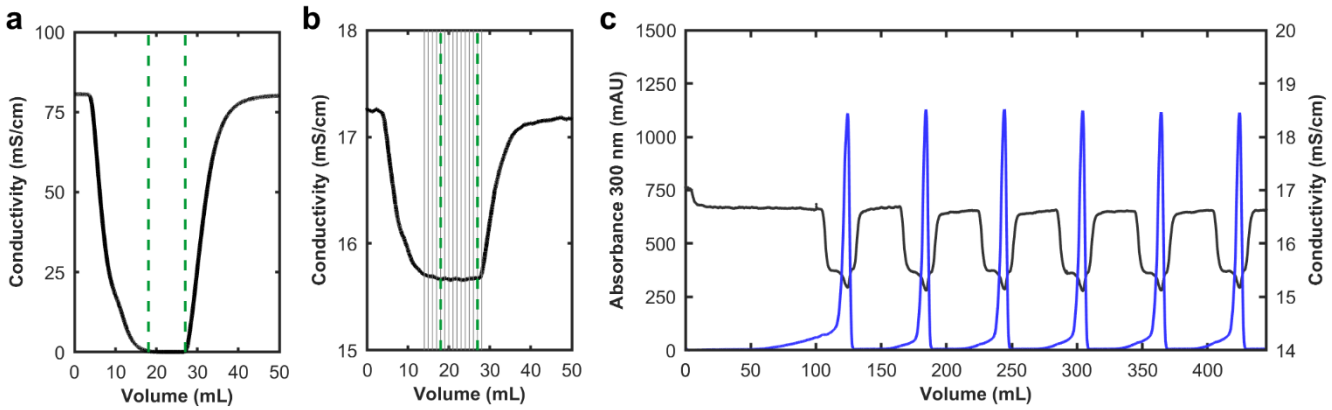
a
b
c
Conductivity (mS/cm)
Volume (mL)
Absorbance 300 nm (mAU)

Fig. 6.

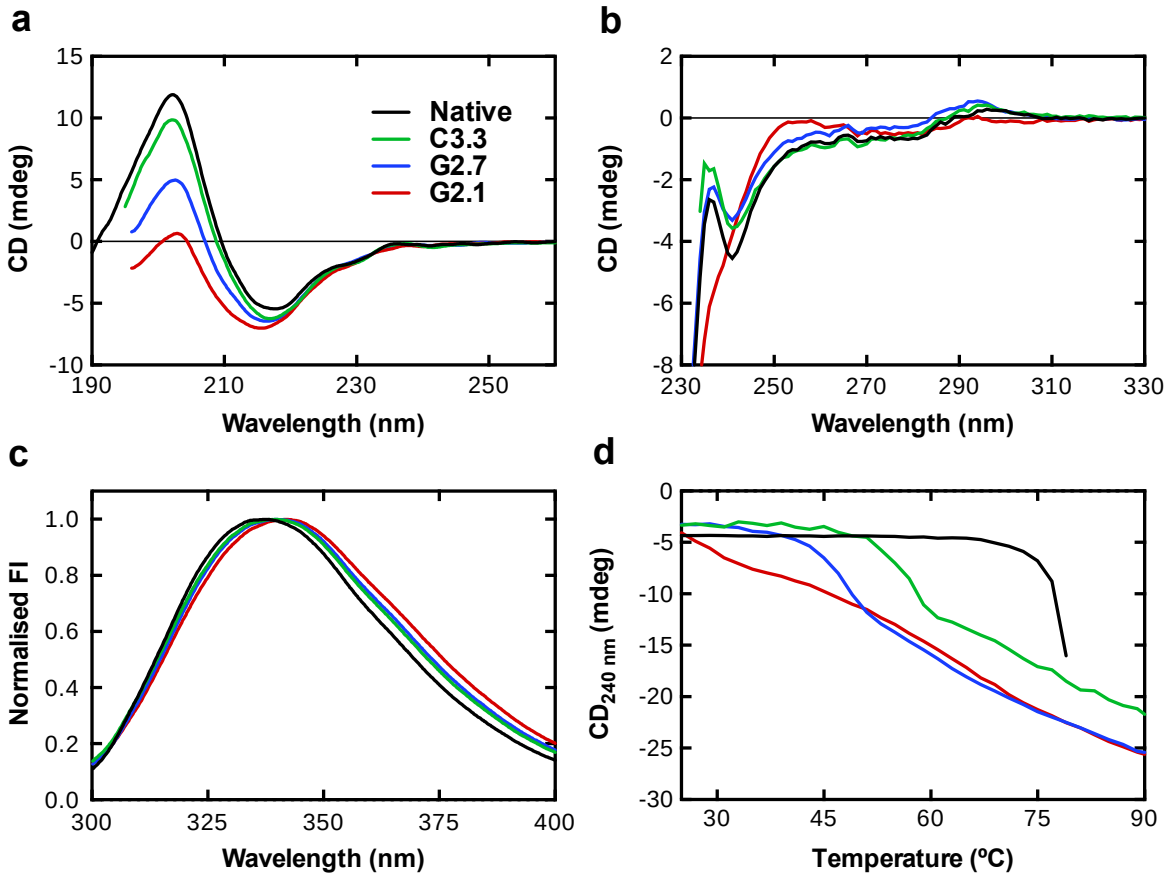
a
b
c
d
Native
C3.3
G2.7
G2.1
CD (mdeg)
Wavelength (nm)
Normalised FI
CD240 nm (mdeg)
Temperature (ºC)

Fig 7.

Figure 1

Click here to download high resolution image

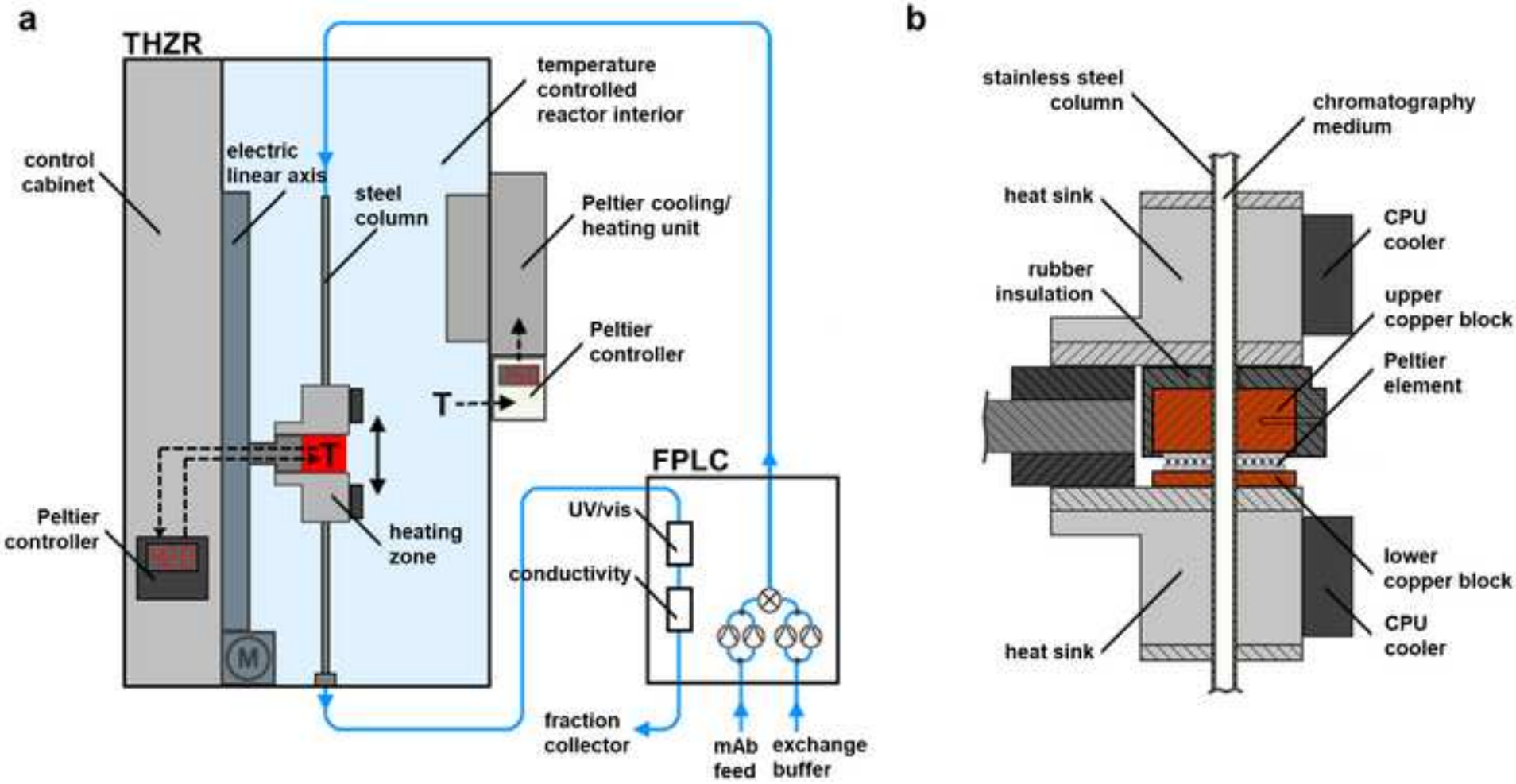

Figure 2

Click here to download high resolution image

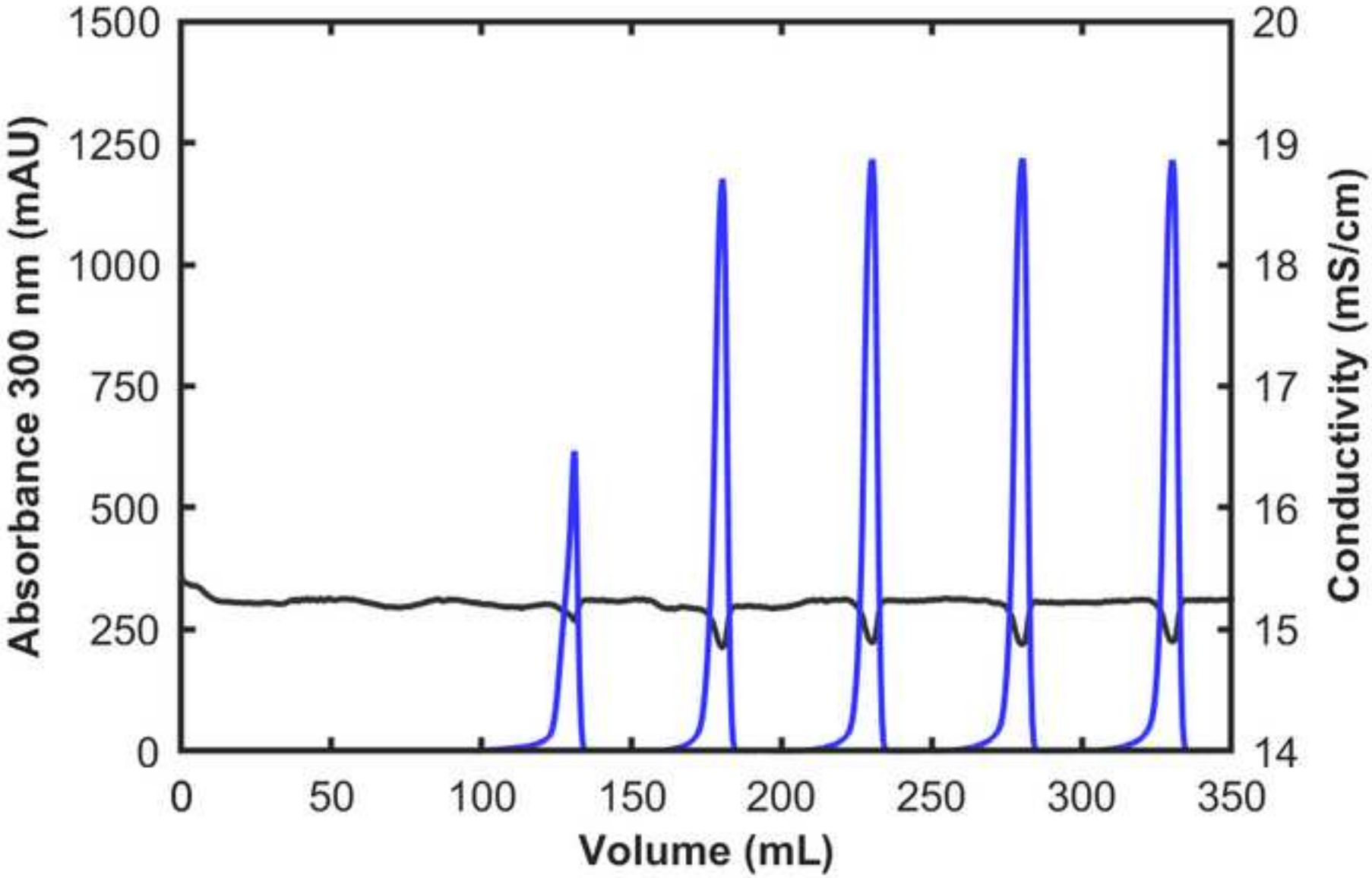

Figure 3

Click here to download high resolution image

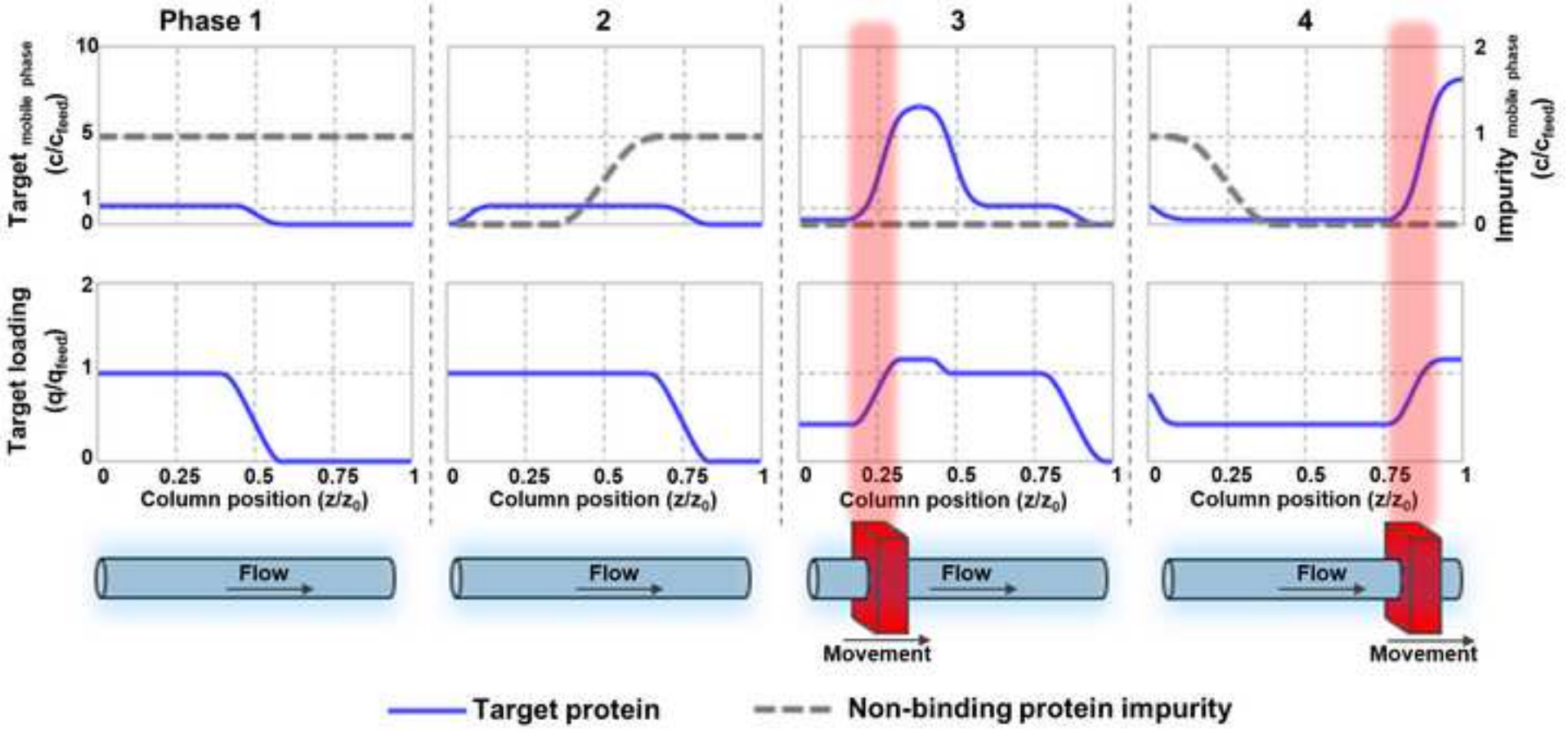

Figure 4

Click here to download high resolution image

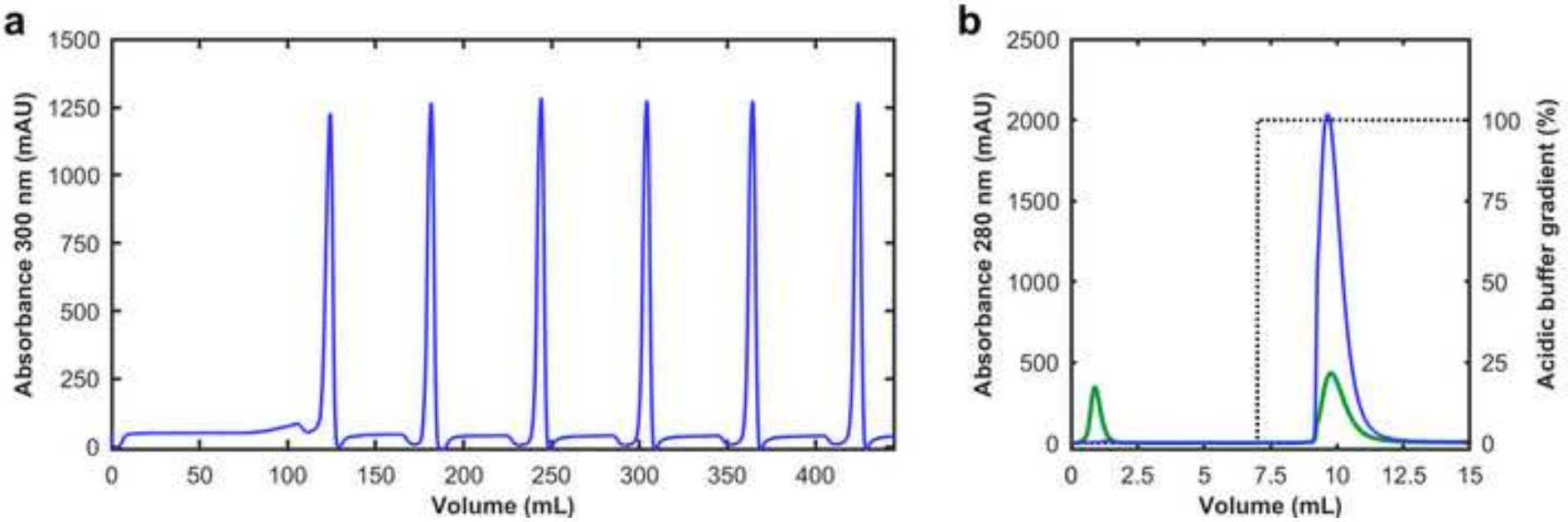

Figure 5

Click here to download high resolution image

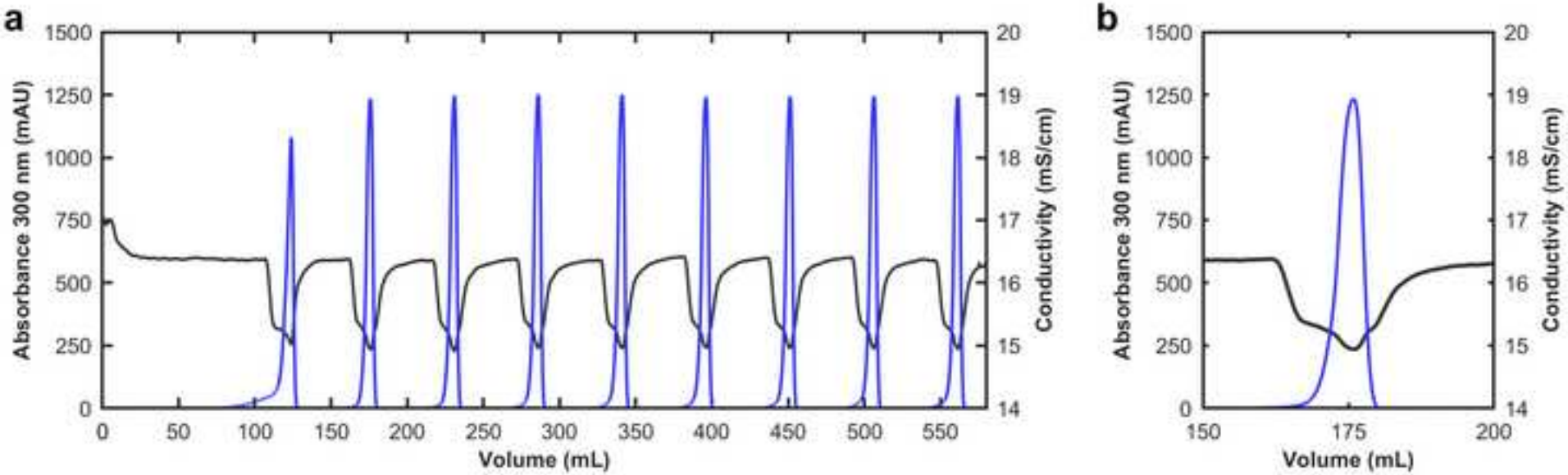

Figure 6

Click here to download high resolution image

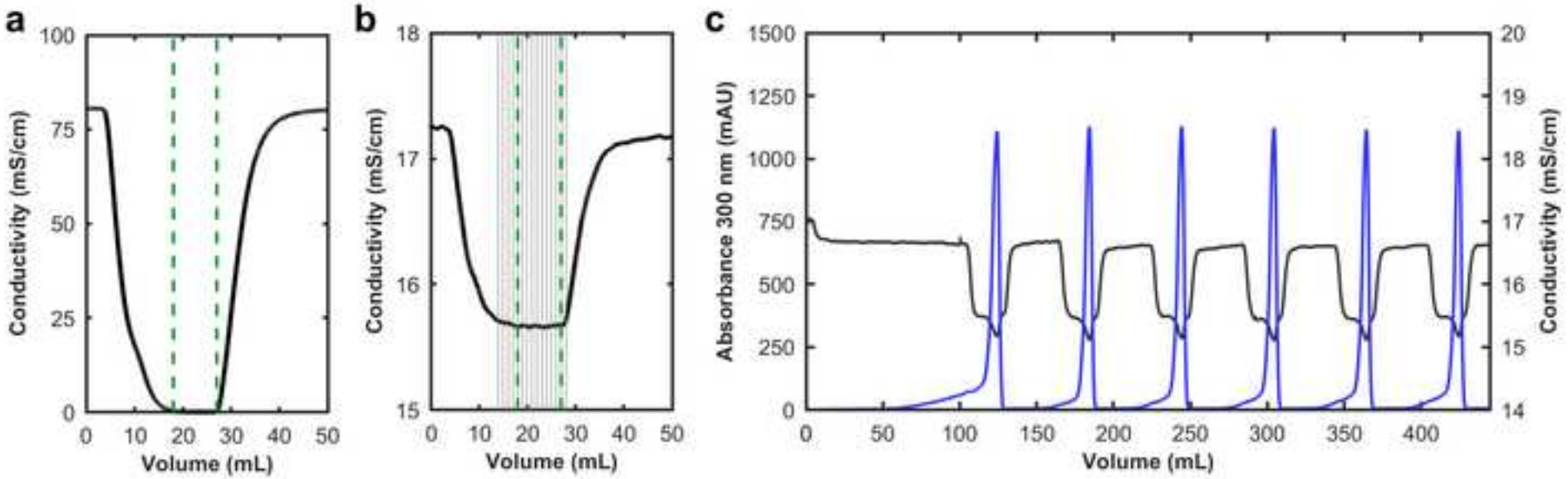

Figure 7

Click here to download high resolution image

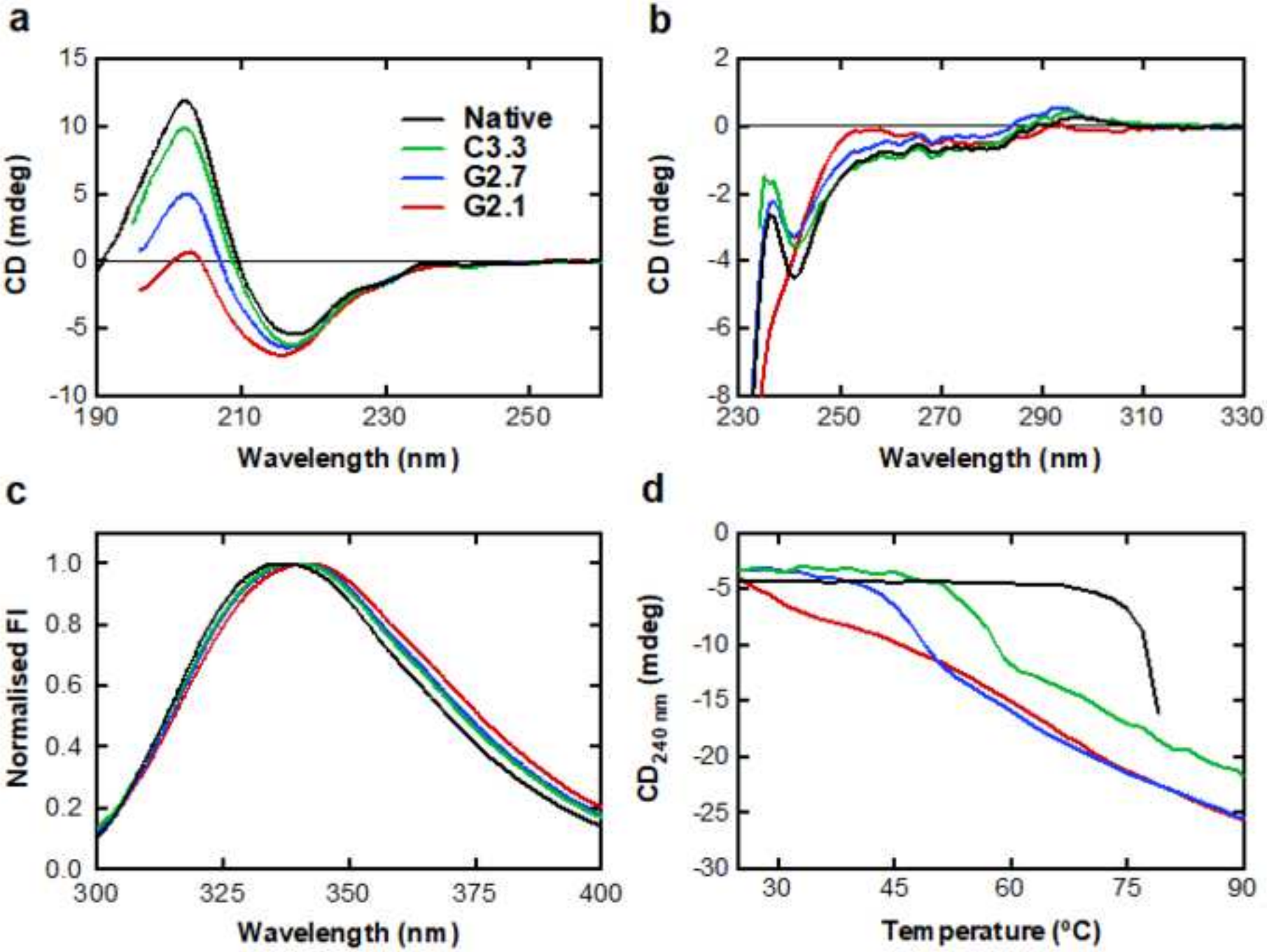

Tables

Table 1. Evaluation of process performance during continuous concentration of mAb corresponding to Fig. 2 (see 2.3.2 and 3.1 details).

Parameter	Peak number(s)					
	1	2	3	4	5	mean 3–5 [a]
Concentration (g/L)	2.3	4.4	5.0	4.7	5.1	4.9
Concentration factor	2.3	4.4	5.0	4.7	5.1	4.9
Volume (mL)	7.9	9.0	8.9	9.1	9.1	9.1
mAb content (mg)	18.5	39.9	45.0	42.5	46.8	44.8
Yield (%)		93.2	93.4	92.7	93.3	93.1
Mass balance (%)		85.2	95.9	91.3	99.9	95.7

[a] Steady-state assumed for peaks 3 to 5.

Table 2. Evaluation of the process performance for the quasi-continuous separation shown in Fig. 4 (see 2.3.3 and 3.2 for details).

Parameter	Peak number(s)						
	1	2	3	4	5	6	mean 3–6 [a]
Concentration (g/L)	5.5	6.1	6.4	6.2	6.4	6.2	6.3
Concentration factor	3.9	4.4	4.5	4.4	4.5	4.4	4.5
Volume (mL)	7.8	6.8	7.0	6.9	6.9	6.9	6.9
mAb content (mg)	43.1	41.9	44.7	43.0	44.3	43.0	43.8
Yield (%) [b]		85.0	90.6	87.1	89.9	87.0	88.7
Purity (%)	95.6	97.1	98.1	98.5	99.0	99.0	98.7

[a] Steady-state assumed for peaks 3 to 6.
[b] Mass balance of 100% assumed.

Table 3. Evaluation of the process performance for quasi-continuous buffer exchange (experiment 1) shown in Fig. 5 (see 2.3.4 and 3.3 for details).

Parameter	Peak number(s)									
	1	2	3	4	5	6	7	8	9	mean 2-9[a]
Concentration (g/L)	3.6	4.9	4.9	4.9	4.9	4.7	4.7	4.8	4.6	4.8
Concentration factor	2.7	3.7	3.7	3.7	3.6	3.5	3.5	3.6	3.4	3.6
Volume (mL)	10.8	8.9	8.9	9.1	9.2	9.2	9.0	9.1	9.1	9.1
mAb content (mg)	39.2	43.5	44.0	44.8	44.8	43.4	42.5	43.9	41.8	43.6
Yield (%)		95.4	95.1	94.8	94.6	94.4	94.2	93.9	93.3	94.5
Mass balance (%)		97.3	98.8	100.8	101.1	98.1	96.2	99.7	95.5	98.4

[a] Steady-state assumed for peaks 2 to 9.